

VILNIUS UNIVERSITY

Jonas Adamonis

HIGH POWER Nd:YAG LASER
FOR PUMPING OF OPCPA SYSTEMS

Summary of doctoral thesis

Physical science, physics (02P)

Vilnius, 2013

Doctoral dissertation was prepared during 2008 – 2012 at Vilnius University.

Scientific supervisor:

dr. Arūnas Varanavičius
(Vilnius University, Physical sciences, Physics – 02 P)

Scientific advisor:

dr. Andrėjus Michailovas
(Center for Physical Science and Technology, Physical sciences, Physics – 02 P)

Doctoral dissertation will be defended in the Council of Physics of Vilnius University:

Chairman:

prof. habil. dr. Valdas Sirutkaitis (Vilnius University, Physical sciences, Physics – 02 P)

Members:

prof. dr. Audrius Dubietis (Vilnius University, Physical sciences, Physics – 02 P)

prof. dr. Artūras Jukna (Vilnius Gediminas Technical University, Physical sciences, Physics – 02 P)

dr. Gintaras Tamošauskas (Vilnius University, Physical sciences, Physics – 02 P)

prof. dr. Rimantas Vaišnoras (Lithuanian University of Educational Sciences, Physical sciences, Physics – 02 P)

Opponents:

dr. Rytis Butkus (Vilnius University, Physical sciences, Physics – 02 P)

prof. habil. dr. Eugenijus Šatkovskis (Vilnius Gediminas Technical University, Physical sciences, Physics – 02 P)

The dissertation will be defended in the Council of Physics at 2 p.m. on September 24th, 2013 in the auditorium Nr. 510 at the faculty of Physics of Vilnius University, Saulėtekio ave. 9, bldg. 3, LT-10222, Vilnius, Lithuania.

The summary of the dissertation was distributed on the 22st of August, 2013.

The dissertation is available at the libraries of Vilnius University and Institute of Physics of Center for Physical Science and Technology.

VILNIAUS UNIVERSITETAS

Jonas Adamonis

DIDELĖS GALIOS PIKOSEKUNDINIS Nd:YAG LAZERIS ČIRPUOTŲ IMPULSŲ
PARAMETRINIŲ STIPRINTUVŲ KAUPINIMUI

Daktaro disertacijos santrauka

Fiziniai mokslai, fizika (02P)

Vilnius, 2013

Daktaro disertacija rengta 2008 – 2012 metais Vilniaus universitete

Mokslinis vadovas

dr. Arūnas Varanavičius
(Vilniaus universitetas, fiziniai mokslai, fizika – 02 P)

Konsultantas

dr. Andrėjus Michailovas
(Fizinių ir technologinių mokslų centras, fiziniai mokslai, fizika – 02 P)

Daktaro disertacija ginama Vilniaus universiteto Fizikos mokslo krypties taryboje

Pirmininkas:

prof. habil. dr. Valdas Sirutkaitis (Vilniaus universitetas, fiziniai mokslai, fizika– 02 P)

Nariai:

prof. dr. Audrius Dubietis (Vilniaus universitetas, fiziniai mokslai, fizika– 02 P)

prof. dr. Artūras Jukna (Vilniaus Gedimino technikos universitetas, fiziniai mokslai, fizika– 02 P)

dr. Gintaras Tamošauskas (Vilniaus universitetas, fiziniai mokslai, fizika– 02 P)

prof. dr. Rimantas Vaišnoras (Vilniaus edukologijos universitetas, fiziniai mokslai, fizika – 02 P)

Oponentai:

dr. Rytis Butkus (Vilniaus universitetas, fiziniai mokslai, fizika – 02 P)

prof. habil. dr. Eugenijus Šatkovskis (Vilniaus Gedimino technikos universitetas, fiziniai mokslai, fizika– 02 P)

Disertacija bus ginama viešame Fizikos mokslo krypties tarybos posėdyje 2013 m. rugsėjo mėn. 24 d. 14 val. Vilniaus Universiteto Fizikos fakulteto 510 – oje auditorijoje. Adresas: Saulėtekio al. 9, III rūmai, LT-10222, Vilnius, Lietuva.

Disertacijos santrauka išsiuntinėta 2013 m. rugpjūčio 22 d.

Disertaciją galima peržiūrėti Vilniaus universiteto ir Fizinių ir technologinių mokslų centro Puslaidininkų fizikos instituto bibliotekose.

Introduction

After the advent of mode-locked laser sources in 1964 [1, 2], the attainable pulse duration decreased and approaches nowadays the ultimate limit of a single field oscillation, which corresponds to ~ 2.5 femtoseconds (10^{-15} s) for visible light [3]. Such ultra – short pulses are required to probe ultra-fast processes in physics [4, 5] and trace primary reaction steps in photo-chemistry and photo-biology [6].

Once terawatt (TW) level intensities of ultrashort pulses were achieved, new range of applications became available in high field physics [7]. For instance, the generation of high order harmonics (HHG) in noble gases allows for the generation of coherent laser like radiation with a wavelength of a few nanometers (XUV) [8]. Furthermore, when using carrier – envelop phase (CEP) stabilized few-cycle driving laser pulses, the generation of isolated attosecond pulses becomes feasible. The shortest pulses generated so far have only 80 as [9] duration.

Shortest pulse laser sources based on Ti:sapphire oscillators with Kerr lens mode – locking producing pulses with duration of 6 – 10 fs and energies of about few nano-Joules are now commercially available. Further amplification of these pulses in linear or regenerative amplifiers are limited up to intensity level of tens of GW/cm^2 due to arising nonlinear effects and optical damage. In order to overcome these limits a chirped pulse amplification (CPA) scheme was proposed by *G. Mourou* in 1985 [10]: low-energy pulses are temporally stretched, amplified in the laser amplifier and subsequently recompressed. By using CPA technology, nowadays the Ti:sapphire laser pulses can be amplified up to terawatt peak power level at repetition rates of 10–50 Hz with an output pulse duration of 18 fs [11]. Shorter pulses are hardly attainable due to limitation caused by spectral gain narrowing effect in Ti:Sapphire amplifiers.

Another technique used for ultrashort pulse amplification is an optical parametric amplification (OPA) [12, 13]. Several unique properties, like negligible thermal load, extremely high single pass gain and broad amplification bandwidth give optical parametric

amplifier a favorable edge over conventional laser amplifiers based on media with population inversion. For high peak power applications (e.g. TW level), the OPA technique is combined with the chirped pulse amplification process. Since the first successful demonstration by Dubietis et al. [14], Optical Parametric Chirped Pulse Amplifiers (OPCPA) have paved the way for a new class of femtosecond optical amplifiers [15]. Typical OPCPA system consist of ultrabroadband signal generator, pulse stretcher, parametric amplifier, pump laser (amplifier) and pulse compressor respectively. The parameters of radiation produced by the pump source is one of the main factor determining system reliability, temporal, spatial and energy characteristics of OPCPA output pulses.

Main objective of this thesis were to develop, investigate and optimize high power Nd:YAG laser system for few optical cycles OPCPA pump.

Main tasks include

- Development of high energy Nd:YAG amplifier comprising of multiple stages of regenerative and linear amplification.
- Investigation of the possibilities to control the duration of the pulses from the picosecond Nd:YAG amplification system seeded by femtosecond pulses.
- Investigation of the amplified picosecond pulse temporal contrast and search of possibilities for pulse temporal contrast enhancement by using of nonlinear optics methods.
- Formation of flat-top pulses at 1064 nm and 532 nm wavelengths by means of cascade second harmonic generation and their amplification in laser amplifiers.

Scientific novelty

A new method for picosecond pulse contrast enhancement based on nonlinear polarization rotation effect in second harmonic crystal has been proposed and investigated.

Formation of smooth temporal profile ~100 ps pulses in Nd:YAG regenerative amplifier seeded by ~60 fs pulses from the Yb:KGW oscillator has been investigated.

It was demonstrated that flat-top pulses, favorable for pumping of OPCPA systems, can be obtained by use of the cascade second harmonic generation.

Practical benefits

The relatively high output energy system of Nd:YAG amplifiers for OPCPA system pump has been developed. By using the output pulses of this Nd:YAG system for OPCPA pump, ultra-broadband (200 nm) pulses were amplified up to 30 mJ of energy. A lot of our proposed technological innovations could be applied for development of commercial picosecond amplifiers, improving their output pulse parameters.

The proposed picosecond pulse temporal contrast enhancement device, implemented in the two stage regenerative amplifier system, could be easily adopted in the other present picosecond systems, amplifying seed pulses of extremely low energy value. Therefore, there is possibility to improve Ti:sapphire oscillator based OPCPA systems, where seed pulses for Nd:YAG amplifiers are formed by using photonic crystal fibers.

Our proposed picosecond pulse envelope shaping method, that is based on pulse temporal profile transformation during second harmonic generation, is particularly suitable for the application in the multistage OPCPA pumped by the second harmonic of Nd:YAG lasers. By applying this method in these OPCPA systems, we could expect to improve temporal and energy parameters of final amplified and compressed pulses.

Major part of our presented results will be implemented in the ultrashort laser facility for national and international access „NAGLIS“ at Vilnius university.

Statements to defend

1. Employment of intracavity Fabry-Pero etalons in two-stage Nd:YAG regenerative amplifier enables for amplified pulse stretching from 60 fs to ~ 100 ps pulse widths. The modulation of amplified pulse envelope is minimal when ratio of thickness of the etalons is around 2, while the stretching ratio and magnitude of envelope modulation can be controlled by changing the reflectivity of etalons.

2. The implementation of second order intensity dependent filter based on the effect of fundamental pulse polarization rotation in unbalanced second harmonic generators and placing it in between of cascades of regenerative amplifier allows for amplified picosecond pulse contrast enhancement without loses in pulse energy. The contrast improvement by $>10^2$ times can be obtained when seed pulse energy is in range of 0,1-10 pJ .
3. The Gaussian pulses from the output of Nd:YAG amplifiers can be transformed into pulses of complex temporal form by using cascade second harmonic generation processes. The flat-top pulses having numerous advantages when used as a pump for OPCPA systems can be obtained by choosing optimum lengths of nonlinear crystals and optimizing pump intensity
4. Employment of optimized regenerative and linear multipass amplifiers, complemented by use of cascade second harmonic generators, allows for realization of effective two channel source of picosecond pulses having both Gaussian and hyper-Gaussian temporal profiles for pumping of OPCPA systems producing several tens of milijoules energy pulses.

Approbation

The result presented in these thesis are published in 3 international scientific ISI -rated papers. Also the results were presented in 6 (3-8 and 11 in the conference list) international and 2 (1-2 and 9-10 in the conference list) national conferences.

The list of author's publications

J. Adamonis, R. Antipenkov, J. Kolenda, A. Michailovas, A. P. Piskarskas, A. Varanavičius, Picosecond pulse contrast enhancement by use of polarization rotation in crystals with the second-order nonlinearity, *Applied Physics B* **106** (2), 321 – 326 (2012).

J. Adamonis, R. Antipenkov, J. Kolenda, A. Michailovas, A. P. Piskarskas, A. Varanavičius, High-energy Nd :YAG-amplification system for OPCPA pumping, *Quantum Electronics* **42** (7), 567–574 (2012).

J. Adamonis, R. Antipenkov, J. Kolenda, A. Michailovas, A. P. Piskarskas, A. Varanavičius, A. Zaukevičius, Formation of flat top picosecond pump pulses for OPCPA systems by cascade second harmonic generation, *Lithuanian Journal of Physics*, **52**(3), 193–202 (2012).

Presentation at conferences

1. J. Adamonis, A. Varanavičius, R. Antipenkov, J. Kolenda, A. Michailovas, Dvipakopis pikosekundinis Nd:IAG regeneratyvinis stiprintuvas su femtosekundinio Yb:KGW osciliatoriaus impulsų užkratu, 38-th Lithuanian National Physics Conference, Vilnius (2009), S4-64.
2. J. Adamonis, R. Antipenkov, J. Kolenda, A. Michailovas, A. P. Piskarskas, A. Varanavičius, Pikosekundinė didelės galios Nd:IAG stiprinimo sistema moduliotos fazės impulsų parametrinio stiprintuvo kaupimui, 38-th Lithuanian National Physics Conference, Vilnius (2009), S4-65.
3. J. Adamonis, R. Antipenkov, J. Kolenda, A. Michailovas, A. P. Piskarskas, A. Varanavičius, Picosecond Nd:YAG amplification system for pumping of high energy OPCPA, Northern Optics 2009, Vilnius (2009), P1-15.
4. J. Adamonis, R. Antipenkov, J. Kolenda, A. Michailovas, A. P. Piskarskas, A. Varanavičius, Picosecond high power Nd:YAG amplifier system for OPCPA pump, Lithuanian – Belarussian seminar “Lasers and optical nonlinearity”, Vilnius (2009).
5. J. Adamonis, R. Antipenkov, J. Kolenda, A. Michailovas, A. P. Piskarskas, A. Varanavičius. Picosecond high power Nd:YAG amplifier system for OPCPA pump, 14th Laser Optics conference (June 28 - July 02, St.Petersburg, Russia)
6. R. Antipenkov, A. Varanavičius, J. Adamonis, A. P. Piskarskas, Development of Sub-10-fs 30 mJ Compact OPCPA System Driven by fs Yb:KGW and ps Nd:YAG Tandem Pump Sources, The 4th EPS-QEOD Europhoton Conference 2010, Hamburg (2010), ThC7.
7. J. Adamonis, R. Antipenkov, J. Kolenda, A. Michailovas, A. P. Piskarskas, A. Varanavičius, Clean 100 ps Pulse Formation and Contrast Enhancement in fs Yb:KGW Oscillator Seeded Nd:YAG Amplifiers, The 4th EPS-QEOD Europhoton Conference 2010, Hamburg (2010), ThP25.
8. J. Adamonis, R. Antipenkov, J. Kolenda, A. Michailovas, A. P. Piskarskas, A. Varanavičius, High energy Yb:KGW and Nd:YAG laser pumped OPCPA system for 10 fs pulse generation at 800 nm, Lithuanian-Belarussian seminar “Laser and optical nonlinearity” Minsk (2011)
9. J. Adamonis, J. Kolenda, A. Michailovas, R. Antipenkov, A. Varanavičius, A. Zaukevičius, Plokščios viršūnės pikosekundinių impulsų formavimaspakopiniuose antros harmonikos generatoriuose, 39-th Lithuanian National Physics Conference, Vilnius (2011), S4-15.
10. A. Varanavičius, J. Adamonis, R. Antipenkov, A. P. Piskarskas, Teravatų galios kelių optinių ciklų impulsų parametrinio stiprinimo sistema lazeriniam kompleksui NAGLIS, 39-th Lithuanian National Physics Conference, Vilnius (2011), S1.
11. J. Adamonis, R. Antipenkov, J. Kolenda, A. Michailovas, A. P. Piskarskas, A. Varanavičius, A. Zaukevičius, Formation and Amplification of Flat Top Picosecond Pump Pulses for OPCPA Systems, CLEO/Europe-IQEC Conf., Munich (2013), CD-P.6.

Author contribution

Author performed all experimental research and data processing, carried out numerical modeling of pulse profile formation in multiple Fabry-Perot etalon system, participated in interpretation of results and discussions, preparation of publications and presented results at conferences.

Contribution of co-authors

A. Varanavičius ir **A. Michailovas** formulated ideas and tasks for experiments, participated in discussions interpretation of results and preparation of publication and conference presentations.

A. Zaukevičius carried out numerical investigation of formation of flat top picosecond pulses by cascade second harmonic generation.

J. Kolenda consulted on designing works of high power picosecond amplifier and accomplished part of these works.

A. P. Piskarskas formulated ideas, participated in discussions.

R. Antipenkov consulted on writing numerical investigation programs and helped to perform experimental measurements by using femtosecond Yb:KGW amplification system.

Thesis summary

The thesis comprises of introduction, six chapters, summary of main results and the list of references.

In the **first chapter** the main requirements for OPCPA pump laser are discussed in detail. We focused on the pump pulse *spectral*, *energetic*, and *temporal* properties, *synchronization* of different lasers which are necessary to develop few cycles TW level OPCPA systems.

In order to amplify few cycles optical pulses, ultra-broadband seed pulse spectrum should be preserved during parametric amplification process in nonlinear crystal. In this case pump pulse wavelength should be properly optimized. Figure 1 shows calculated gain spectra of a type-I β -BaB₂O₄ (BBO) crystal for several pump wavelengths [16]. In case of the 400 nm pump (SH of an ordinary Ti:sapphire laser) the gain spectrum is broadest (from

520 to 750 nm Fig. 1(a)), supporting sub-5-fs operation, which is fully covered by the white light continuum seed (b).

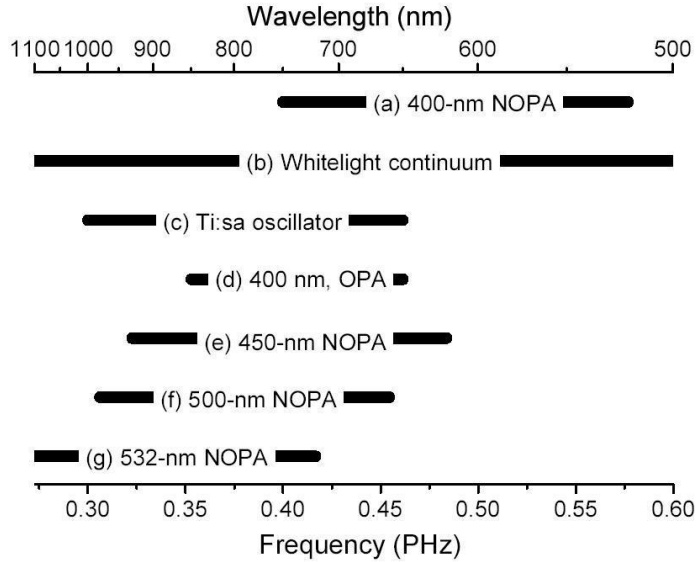


Fig. 1. Calculated parametric gain spectra of a BBO crystal for several pump wavelengths. Noncollinear and phase-matching angles for the calculations are optimized to achieve broadest gain bandwidth for each pump wavelength [16].

However, the spectrum of a typical broadband Ti:sapphire oscillator (c), when used as the seed source of OPCPA systems, has poor spectral overlap with 400 nm pumped BBO's spectral acceptance shown in (a). On the other hand the pump wavelength of 450-532 nm is suitable to amplify the seed pulses from Ti:sapphire oscillators (see (c) and (e)-(g)), allowing to produce few cycle pulses. This pump wavelength requirement could be fulfilled by using SH output pulses from Nd^{3+} or Yb^{3+} ions doped laser amplifiers. Diode pumped Yb doped lasers ($\lambda=1030$ nm) and amplifiers having a low quantum defect of only a few percent, are suitable for high average power few cycles OPCPA systems [17]. Recently, there are a lot of efforts to boost Yb amplifiers up to hundreds of millijoule [18] or even several Joule [19] pulse energy level, required for pumping TW power OPCPA systems. However, despite of the rapidly growing Yb laser technology, the TW pulse peak power level OPCPA, pumped by Yb amplifier pulses, hasn't been demonstrated yet. On the other hand, several few cycles TW level OPCPA systems pumped by SH pulses produced by well developed and reliable Nd^{3+} doped amplifiers are already presented [20, 21]. The most

powerful few cycles (7.7 fs) OPCPA system designed up to date, delivered pulses with 16 TW peak power [21]. This system was pumped by 1 J frequency doubled (532 nm) pulses, extracted from Nd:YAG amplifiers. Note, that PW level OPCPA systems with a longer output pulse duration ($>30 - 40$ fs) was pumped by Nd³⁺ doped amplifiers (Nd:YLF and Nd:glass) as well [22, 23].

Unlike gain media with inversion storage, in OPCPA systems a severe challenge of ensuring strict synchronization between the pump and seed pulses arises. The timing precision within a fraction of the pulse durations is required because of the instantaneous energy exchange in parametric three-wave mixing. An ideal solution for full optical synchronization is seeding both the OPCPA and its pump laser by using common ultrashort pulse oscillator. Few cycles (5.5 fs) OPCPA seeded from a Ti:sapphire oscillator and pumped by the second harmonic of a Ti:sapphire amplifier (that was also seeded by the same oscillator) was demonstrated [16]. Nevertheless scaling up the output of Ti:sapphire laser amplifier was limited by high level of amplified stimulated emission (ASE) [16]. Furthermore high energy Ti:sapphire amplifier systems are very complex, because each amplification stage requires of its own pump source – a green Q-switched ns laser.

It is possible optically synchronize Nd³⁺ pump amplifiers with ultra broadband OPCPA seed source by using octave-spanning (550 nm – 1,2 μ m) Ti:sapphire oscillator [24, 25]. However, these oscillators, based on highly advanced broadband chirped mirrors, cannot ensure several picojoule energy level within the bandwidth of a typical picoseconds regenerative amplifier. Such level of the injected seed is required to compete efficiently with the ASE in the picosecond amplifier. As a result, in these amplifiers ASE sets up a significant part (up to 10%) of the overall amplified output pulse energy [25].

Nonlinear optics methods reveal another possibility for optical synchronization of ultra-broadband (e.g. Ti:sapphire) oscillator and Nd³⁺ (or Yb³⁺) amplifiers by shifting Ti:sapphire amplifier output pulse wavelength toward Nd³⁺ amplifier emission line (1064 nm) by using different frequency generator [26]. In case of the unamplified oscillator pulses, parametric frequency shifters are extremely inefficient. However a fraction of broadband oscillator pulse spectrum could be frequency-shifted in a photonic crystal fiber (PCF) through

phenomenon called soliton self-frequency shift (SSFS) [27]. By applying this technique, oscillator output beam should be confined to very small diameter (1.8 μm) fiber core. As a result, reliability of this method is limited by thermo-mechanical instabilities.

Instead of using a single ultra-broadband source delivering pulses with spectrum that covers the entire frequency range supported both by the OPCPA gain and the picosecond laser gain, some groups investigated possibility to synchronize laser oscillators operating at different wavelengths. One possibility of realizing a two-color scheme is to employ self-stabilization of two mode-locked oscillators, lasing at the seed and pump wavelengths respectively, via a nonlinear optical (Kerr-lens) mechanism [28]. In terms of complexity, however, this method is not easier to implement, especially in the solid state oscillators. Application of the active electronic synchronization, based on GHz electronics, is another way to synchronize ultra-broadband Ti:sapphire oscillator with the master oscillator of a picosecond OPCPA pump Nd^{3+} amplifier [20]. Although less than 1-ps synchronization is possible by electronic phase lock loop (PLL) stabilization of the cavity lengths of the pump and seed oscillators [29], this system is fairly complex and its long-term stability has not yet been proven.

As it follows from our discussion, either passive or active synchronization of ultra-broadband Ti:sapphire with Nd^{3+} pump amplifier is a complicated task. For this reason some scientific groups showed an alternative way in developing few cycle OPCPA systems. In these works instead of Ti:Sapphire oscillator, Yb:KGW master oscillator ($\lambda=1030$ nm) was used [30, 31]. Output spectrum of Yb:KGW pulses partially overlapped with Nd:YAG amplifier emission line ($\lambda=1064$ nm). Thus full-optical synchronization of Yb:KGW oscillator and Nd:YAG amplifier was realized, while ultra-broadband OPCPA seed was generated by pumping a white light continuum generator (WLC) with first [31] or second [30] harmonic of Yb^{3+} amplifier output pulses. Using this approach few cycle OPCPA systems operating in the near and mid infrared spectral region were demonstrated with a maximum output pulse peak power of 90 GW [31]. TW level few cycle OPCPA system based on single master Yb:KGW oscillator is under construction in Vilnius University as well. The most of the tasks presented in this thesis are addressed to develop and optimize the OPCPA pump

amplifiers parameters, including pulse temporal characteristics. Nowadays the duration of the pump pulses in OPCPA systems ranges from ~ 1 ps to several ns. The most powerful [23] PW level and efficient [32] OPCPA systems designed up to date are pumped by nanosecond pulses. Nevertheless, nanosecond pump pulses are rather unattractive for few cycles OPCPA. Firstly, the parametric gain and its bandwidth are determined by the combination of pump intensity and crystal thickness which cannot exceed 4–5mm for few-cycle amplifiers [25]. Therefore, efficient (10-20 %) broadband amplification calls for the high pump intensity (10 GW/cm^2). The damage threshold intensity for nanosecond pulses (1 GW/cm^2) is lower than for tens of picosecond pulses (20 GW cm^2), which makes the latter a more favorable choice. Secondly, the temporal seed stretching ratio, which is needed to match the pump and seed pulse durations, and allow effective recompression in view of high order dispersion terms, typically is limited to 10^3 - 10^4 [33]. That means that the pump pulse duration should be in the 10-100 ps range.

In OPCPA, the efficiency of the amplification process strongly depends on the pump pulse shape and the ratio between the pump and seed pulse durations [34]. If a seed pulse is much shorter than the Gaussian shape pump pulse, only a small part of the pump light will be utilized for amplification, resulting in a low efficiency. The amplified bandwidth will be broad in this case, as the entire seed spectrum overlaps with the peak of the pump pulse, leading to a short pulse duration. Stretching the seed pulse will initially provide a strong rise in efficiency, as the overlap with the pump pulse improves. However, as the seed pulse is stretched more, the edges of its spectrum shift away from the peak of the pump pulse and will experience a lower gain, resulting in spectral narrowing and a longer compressed pulse duration. In the demonstrated few cycles OPCPA, the ratio between pump and seed pulse durations varies from 6 [20] to 2.5 [21]. The temporal overlap between pump and seed pulses also influences amplified and compressed pulse contrast, defined as the ratio between the pulse peak intensity and the intensity of the amplified parametric superfluorescence. Since an imperfect overlap will lead to the generation of fluorescence at those points in time, where there is no or only very little seed light available [35]. Clearly, a rectangular shape for the pump pulse would be the optimal temporal profile for OPCPA, providing

equal gain at any point in time, making optimal use of the available pump energy [36] with a lower level of amplified pulse contrast deterioration. It also has been found that temporal modulation and random noise on the pump pulse can translate into significant pedestal on the final recompressed pulse [37]. Temporal modulation of the pump pulse could be either, due to high level of ASE [37] or due to the pump amplifier intra-cavity Fabry-Perot etalon effect. Following the considerations about pump pulse duration and temporal profile contribution to overall OPCPA efficiency, we dedicated the **second chapter** of the thesis to pump pulse profile formation. In our system femtosecond seed pulses from Yb:KGW have been temporally stretched due to gain narrowing in the regenerative amplifier (RA) and use of Fabry-Perot intracavity etalons (IEs). It is worth mentioning that if IE double pass transit time is on the order of the input pulse duration, the RA output pulse could be temporally modulated [38]. In order to avoid this modulation multiple IEs with different thicknesses are usually used. In order to examine the impact of single or double IE systems on the amplified pulse envelope, we performed computer modeling using the algorithm presented in [38]. The pulses in simulations were described as Gaussian ones, their phase modulation was accounted for by a linear chirp factor γ which enters the uncertainty relation for a transform-limited pulse: $K = \Delta\nu \times \Delta\tau = 0.44 \times \sqrt{1 + \gamma^2}$. In a real picosecond RA $\gamma \neq 0$ due to nonlinear effects in RA cavity components. Several pulse duration formation setups were tested experimentally and theoretically. The measurements were performed with the help of third order cross-correlator using ~ 300 fs frequency doubled pulses from Yb:KGW RA as a probe. At first stage of the experiment, 25 ps (FWHM) output pulses from RA1 were injected to the RA2 cavity, containing a 2-mm-thick single IE made of SF-6 glass with 20 % reflection coatings on both surfaces, and after 9 round trips were amplified up to 100 μ J. For this particular case, the input pulse duration was close to the IE double transit time (24 ps). As a consequence, the RA2 output pulse exhibits severe temporal envelope modulation (up to 0.12) which is in a good agreement with simulation results (Fig. 2).

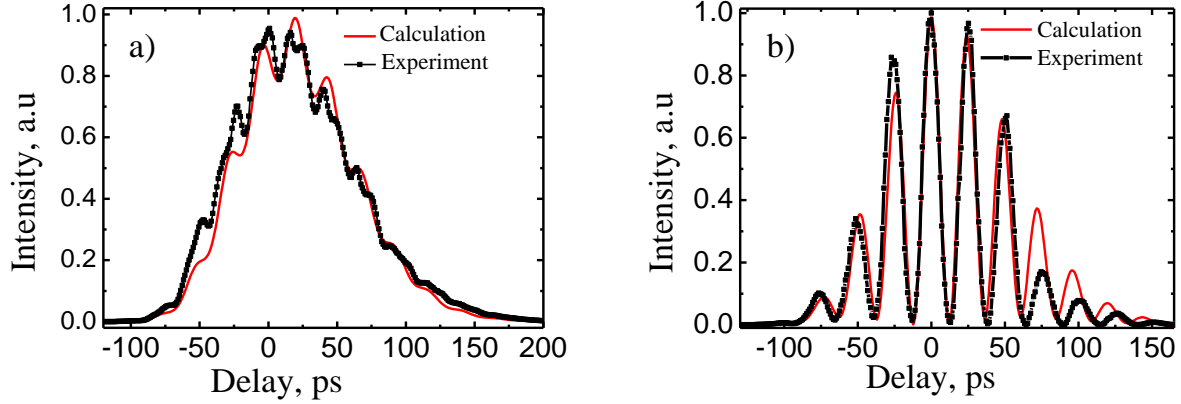


Fig. 2. Pulse temporal profile at the output of RA2 with a single 2-mm-thick SF-6 glass intracavity etalon ($R_1 = 0.2$) when the etalon is tilted to resonant (a) and antiresonant position (b). In calculations the linear chirp factor $\gamma = 1$ is used, the number of round trips in the RA2 is 9.

Computer modeling revealed that temporal envelope modulation strongly depends on the seed pulse duration $\Delta\tau$ (Fig. 3a). Virtually varying the input pulse length $\Delta\tau$ from 20 ps to 32 ps, envelope modulation was reduced from 4×10^{-2} to 6×10^{-5} at $\gamma = 0$. On the other hand, the calculation shows that the magnitude of envelope modulation is strongly affected by the input seed pulse chirp γ . When $\gamma = 1.1$ and $\Delta\tau = 32$ ps, the modulation depth is 0.5×10^{-2} . This value is three orders of magnitude worse than $\gamma = 0$. The employment of the second IE in the RA cavity made it possible to reduce undesired pulse modulation (Fig. 3b).

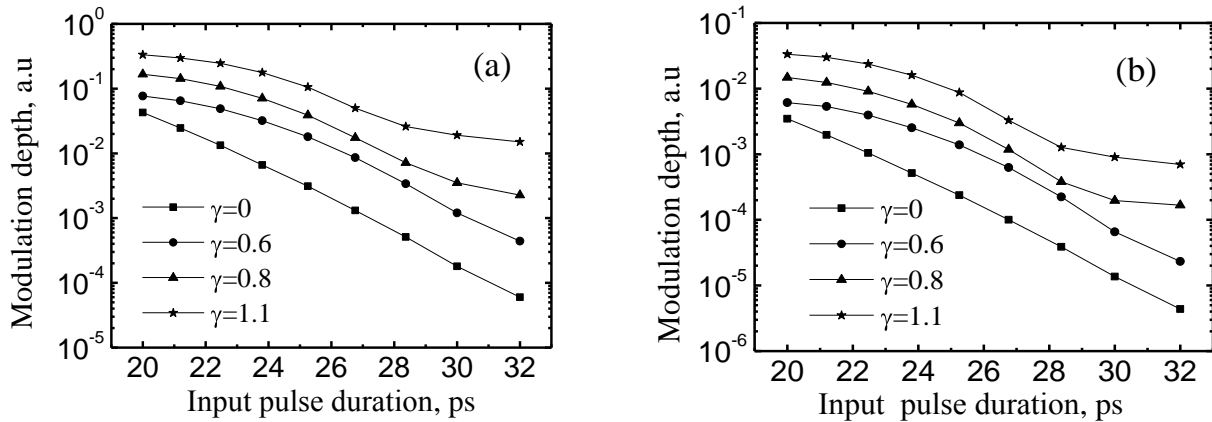


Fig. 3. Calculated pulse intensity envelope modulation depth versus input pulse duration and linear chirp parameter γ for a single 2-mm-thick SF-6 glass etalon ($R_1 = 0.2$) (a) and an additional second 1-mm-thick SF-6 etalon ($R_2 = 0.07$) (b). The number of round trips in the RA2 is 9.

According to calculations, insertion of an additional 1-mm-thick uncoated IE (SF-6) could result in the pulse envelope modulation reduction from 0.5×10^{-2} to 7×10^{-4} . The calculated

dependence of the pulse envelope modulation depth on the second IE thickness and reflectivity R_2 is presented in Fig. 4. As seen from Fig.4a, the optimum thickness of the second IE should be equal to half the length (1 mm in our case) of the first etalon.

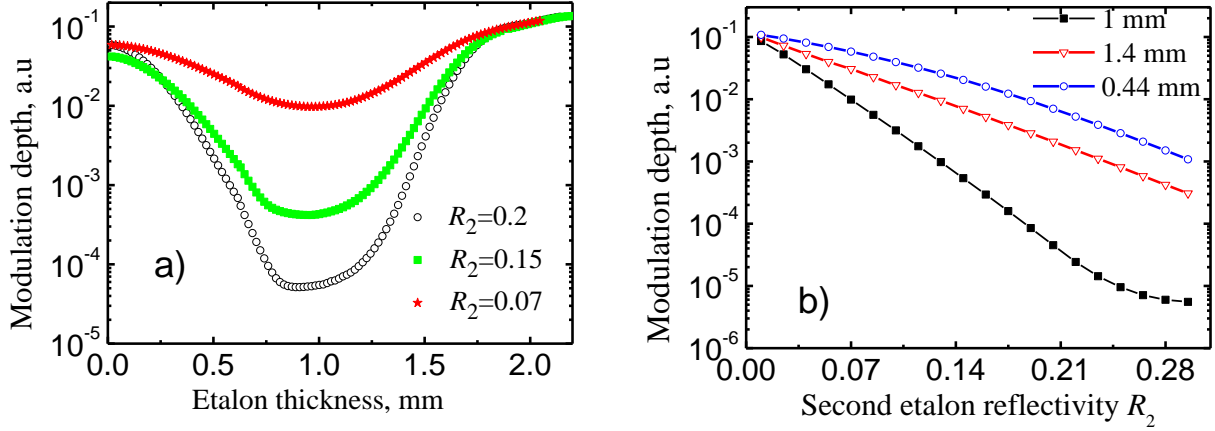


Fig. 4. Calculated pulse envelope modulation depth versus the second intracavity etalon thickness (a) and surface reflectivity R_2 (b). The input pulse duration is 25 ps, the chirp parameter is $\gamma=1.1$, the number of round trips is $n=9$, the first intracavity SF-6 etalon thickness is 2 mm, the reflectivity is $R_1=0.2$.

Another important IE parameter which impacts the modulation depth is IE surface reflectivity R_2 . The increase in R_2 results in significant reduction of the modulation depth (Fig. 4b). It should be noted that introducing the second IE also affects the output pulse duration. However, the impact of the second IE on the pulse lengthening is quite weak compared with the contribution of the first IE. For instance, with changing 1-mm-thick IE reflectivity of from 0.04 to 0.3 the output pulse width increased from 95 ps to 115 ps (without accounting for gain narrowing). On the basis of simulation results we inserted into the RA2 cavity two SF-6 etalons: the first one was 2-mm thick with 0.2 reflectivity and the second one was 1-mm thick with 0.3 reflectivity. By using this double IE system, the RA1 output pulse was stretched in time up to 100 ps without noticeable pulse modulation. According to computer simulation, the modulation depth value should not exceed 5.5×10^{-6} . Unfortunately, in the experiment the noise of photomultiplier did not allowed us to reach the required accuracy.

The presence of ASE is an overall problem for most Nd^{3+} OPCPA pump amplifiers which are full-optically synchronized with a femtosecond (Ti:Sapphire, Yb:KGW)

oscillators. The energy of the seed pulses from fs oscillator usually is low (pJ level) and the high gain regenerative amplifiers are used for boosting it to the μJ or mJ energy levels, sufficient for the amplification in linear power amplifiers. A regenerative amplifier produces output in the form of amplified picosecond pulse and nanosecond background caused by amplified spontaneous emission. An insufficient signal-to-ASE background contrast ratio at the output of OPCPA pump amplifiers may severely reduce the total efficiency of the OPCPA systems. Thus, in the **third chapter** of the thesis we presented a picosecond pulse cleaning technique based on intensity-dependent fundamental pulse polarization rotation in type II phase-matching second harmonic generator operated under the conditions of unbalanced intensities of input polarization components. The polarization rotation is driven by the second-order nonlinear process, and therefore the optimum operation conditions can be achieved at relatively low intensities ($<1\text{GW}/\text{cm}^2$) of incident radiation. The use of this effect for realization of the device exhibiting intensity-dependent transmission has been demonstrated for the first time by Leford and Barthelemy [39] and has been employed in setups of the all-optical transistor [40] and various mode locking schemes [41–43]. But to our knowledge, it is the first time such a technique has been implemented for the contrast enhancement in picosecond pulse amplifiers. Initially the performance of the intensity-dependent transmission filter has been tested in the setup presented in Fig. 5.

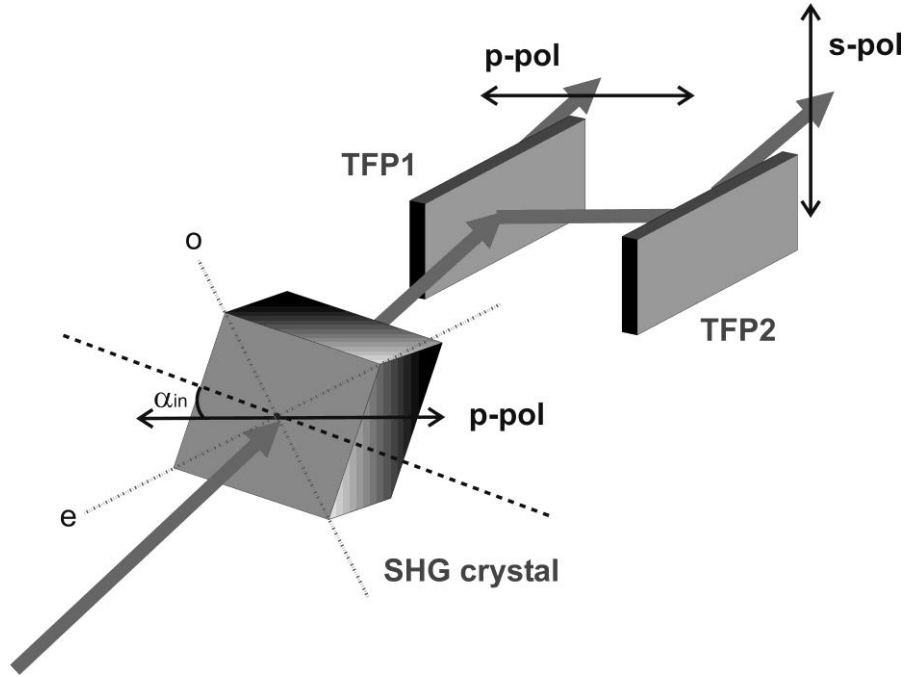


Fig. 5 Setup of nonlinear filter. TFP1 and TFP2 are thin-film polarizers.

In this setup, linearly polarized pump radiation was directed to the second harmonic generation (SHG) crystal which was cut for type II frequency doubling. The KTP crystal cut for SHG at polar angle $\theta=90^0$ and azimuthal angle $\varphi=23.5^0$ was used for SHG. The second harmonic conversion efficiency in this type of the crystal and the final state of pump polarization at the output are dependent both on the pump intensity and the angle between pump polarization plane and polarization directions for the ordinary (o) and extraordinary (e) waves in the SHG crystal. In case when the angle α_{in} between pump polarization plane and bisector of the angle between crystal indicatrix axes (dashed line in Fig. 5) is zero, the two orthogonally polarized pump waves of equal amplitude are propagating in nonlinear crystal. During process of SHG these components are depleted by the same ratio and, as a result, there is no change in state of fundamental radiation polarization. When $\alpha_{in} \neq 0$, the amplitude of o-polarized and e-polarized pump components differs. SHG diminishes both components by the same amount and, as a consequence, resultant pump polarization remains linear but experiences rotation of its direction. The degree of polarization plane rotation is a function of SHG efficiency, i.e. is intensity dependent. With the polarizer installed after the SHG crystal, such a setup exhibits intensity dependent transmission and

could serve for enhancement of the contrast between main pulse and background radiation or possible satellites. The filter operation was tested using Nd:YAG laser generating 100 ps (FWHM) and 50 μJ pulses at 1064 nm. The laser beam was focused to waist of an approximately 500 μm diameter (at $1/e^2$ intensity level) located in the KTP crystal resulting in maximum radiation intensity of 0.25 GW/cm^2 . The capability of the device to discriminate between high intensity pulses from low intensity signal (noise) was checked by measuring the pulse cleaner transmission as a function of incident pulse energy at different values of α_{in} . The measurement data for the KTP crystals of length 7 and 3 mm are presented in Fig. 6a and 6b. The zero value of angle α_{in} was designated to the case when the pump polarization plane makes 45° with the crystal indicatrix axis, i.e. at the crystal orientation providing highest SHG conversion. The maximum induced transparency of 28% was obtained at the angle $\alpha_{\text{in}}=12^\circ$ and fundamental pulse intensity of 0.23 GW/cm^2 using the 7-mm KTP crystal. In accordance with theory [39], the increasing of α_{in} results in induced transmission saturation at lower peak intensities, but the maximum transmission value becomes lower. For the 3-mm KTP crystal the maximum observed filter transmission did not exceed 3.5 %. Lower transmission values were caused by the reduced nonlinear interaction length resulting in lower degree of polarization rotation. The main parameter defining the efficiency of the pulse cleaner is a contrast enhancement factor. The magnitude of this factor for our setup was calculated as a ratio of measured filter transmission for the incident pulse of intensity 250 and 1 MW/cm^2 . We should note that for the pulse intensities below 1 MW/cm^2 the changes in filter transmission caused by the polarization rotation were undetectable due to the presence of background radiation leaking through the polarizers.

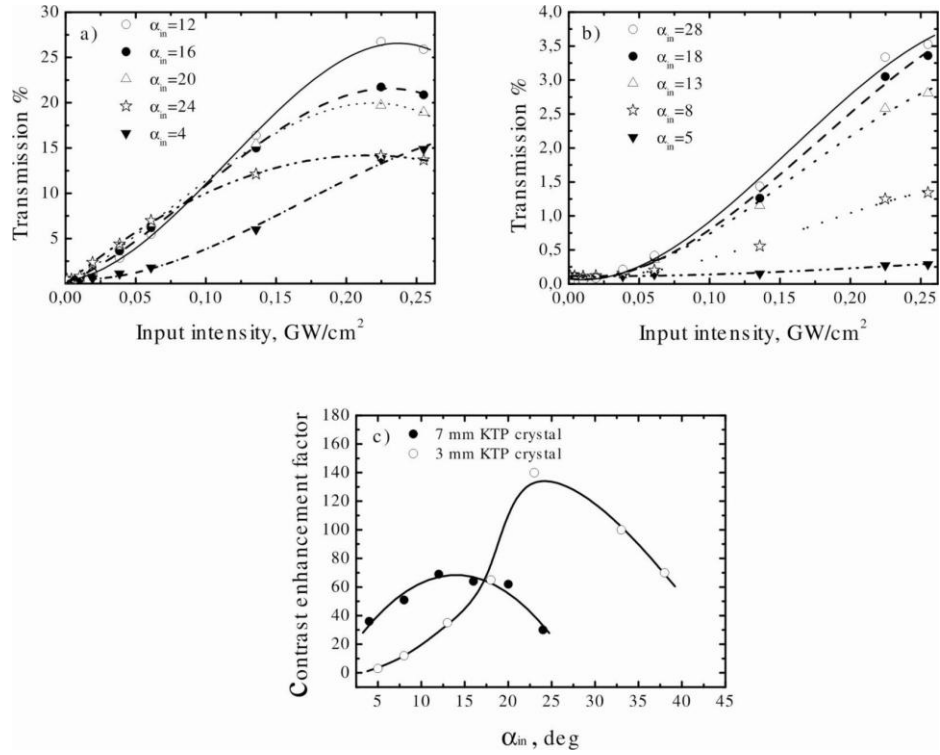


Fig. 6 Dependence of energy transmission of the nonlinear filter on input pulse intensity for different values of α_{in} for KTP crystals of (a) 7 mm and (b) 3 mm lengths. (c) Dependence of contrast enhancement factor on the KTP crystal orientation. In all pictures the *lines* are the guides for the eyes.

The contrast ratio dependence on angle α_{in} is presented in Fig. 6c. The maximum values of the contrast enhancement factor for 3- and 7-mm crystals are 140 and 70, respectively, and they are obtained at different angles α_{in} . The test results allowed predicting the contrast ratio enhancement by at least two orders of magnitude in the real system application. The tested nonlinear filter was implemented in the two-stage 1-kHz-repetition-rate picosecond regenerative amplifier system with the pulse cleaner placed in between RA1 and RA2 (Fig.7). This regenerative amplifier system was specially developed for OPCPA pump and is described in detail in the sixth chapter of this thesis. The regenerative amplifiers were seeded with 60 fs pulses from the laser diode pumped Yb:KGW femtosecond oscillator (Light Conversion, Ltd.) and were used as a preamplifier in the pump channel of the high energy OPCPA system described in the sixth chapter of the thesis.

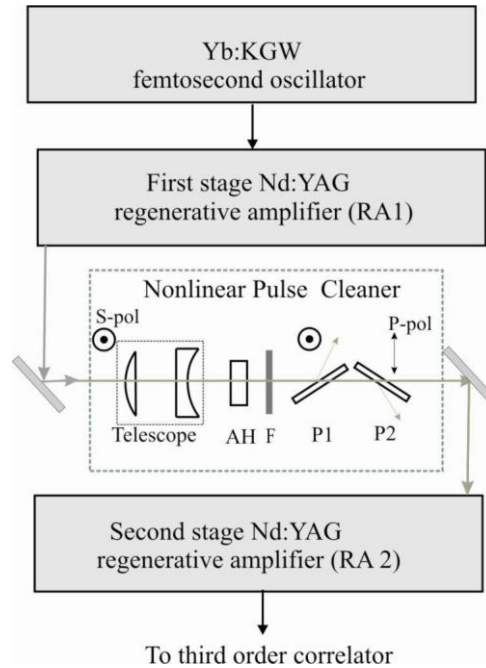


Fig. 7 Schematic of the picosecond pulse amplification system. P1, P2—thin film polarizers, AH—second harmonic KTP crystal, F—the second harmonic cut-off filter.

The maximum energy of the in RA1 amplified pulses of 45 μJ was limited by the damage of the Nd:YAG crystal. The temporal pulse characteristics were measured with the third-order cross correlator (Sequoia, Amplitude Technologies) designed for 1000–1150 nm wavelength range, which assures femtosecond pulse contrast measurements with the dynamic range of $\sim 10^{11}$ in the time span of 600 ps. For the amplified pulse contrast enhancement the beam from RA1 was directed to the pulse contrast cleaner. The incident beam diameter was reduced by the telescope and the collimated beam diameter in the 3 mm KTP crystal was set to $\sim 500 \mu\text{m}$ (at $1/e^2$ intensity level) resulting in the maximum peak intensity of $0.88 \text{ GW}/\text{cm}^2$. The polarization of fundamental radiation after the SHG crystal was analyzed by a pair of thin-film polarizers while the second harmonic was cut with the color glass filter. In this setup we succeeded to reach the nonlinear filter maximum transmission of 24 % at an angle $\alpha_{\text{in}}=15^\circ$. The increase in the filter transmission compared to previously described test experiments can be explained by higher incident pulse intensity. The employment of the intensity-dependent nonlinear filter ensured the pulse contrast enhancement by more than two orders of magnitude. The measured cross-correlation trace

presented in Fig. 8a indicates that ASE intensity was lowered down to $\sim 2 \times 10^{-9}$ with reference to the main pulse amplitude. We also note the reduction of the transmitted pulse duration by $\sim 23\%$ due to the nonlinear system response (Fig. 8b).

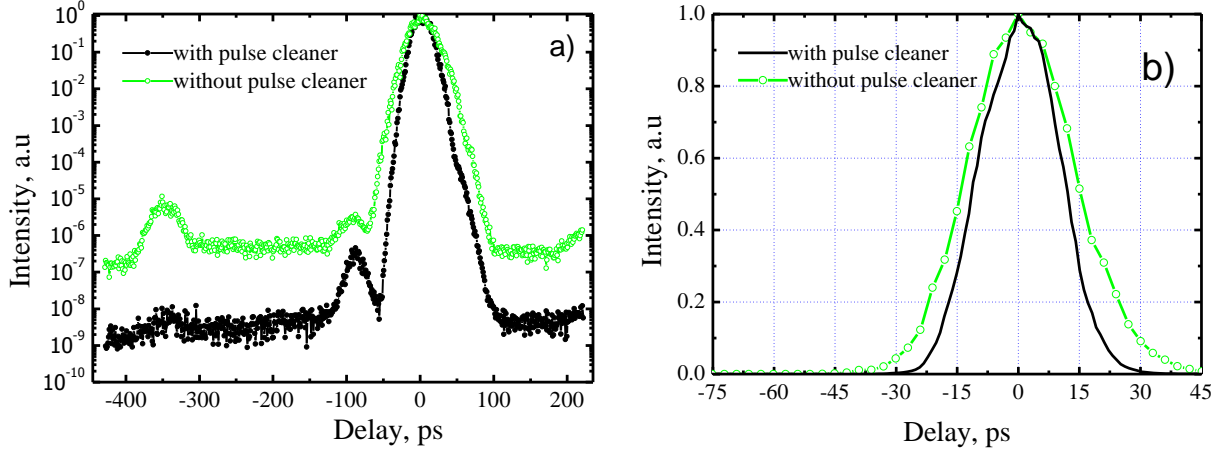


Fig. 8 The third-order cross-correlation traces of the pulses amplified in the first-stage RA1 plotted in (a) logarithmic and (b) linear scales both with and without a pulse cleaner.

Unavoidable losses introduced by the nonlinear filter have been easily compensated in RA2. Output pulses of RA1 after the nonlinear filter were injected into RA2 and amplified up to 100 μJ level which was limited by the available pump power. The high dynamic range cross-correlation of RA2 output pulses is presented in Fig. 9a.

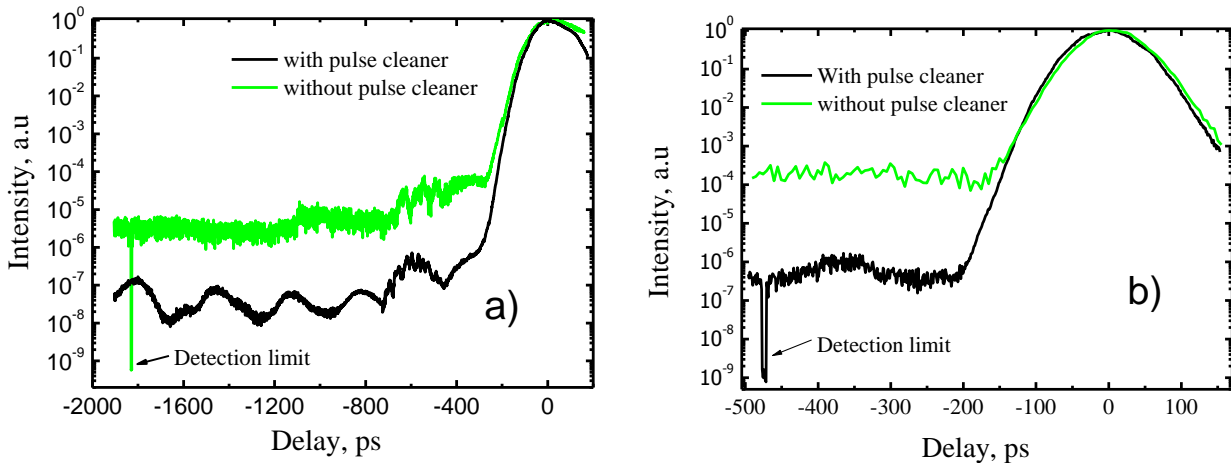


Fig. 9 The third-order correlation traces at the output of RA2 with (a) seed from Yb:KGW oscillator and (b) seed from Ti:sapphire oscillator with PCF frequency shifter

The ASE intensity level of 3×10^{-6} in respect to the main pulse intensity was detected when the nonlinear filter was not used. With employment of pulse cleaner the ASE intensity level fell down by more than two orders of magnitude revealing slow modulation of background radiation that in our opinion is caused by action of intracavity etalons. The measured ASE to main pulse contrast ratio of $\sim 1.5 \times 10^{-8}$ indicates certain pulse contrast degradation as compared to the contrast value after the nonlinear filter (see Fig. 8a) resulting from gain saturation and spontaneous emission in the active element of RA2. Due to the same reasons further pulse amplification in high energy linear amplifiers leads to slight drop in the main pulse/ASE contrast ratio. At maximum output energy of 600 mJ the ASE/pulse intensity ratio is 4×10^{-8} (not presented here). The performance of the pulse cleaner has also been tested for the case of significantly lower seed pulse energies at the input of regenerative amplifiers. The femtosecond Ti:sapphire oscillator generating pulses with spectrum covering 670–950 nm was used as a seed source for Nd:YAG RA. The spectrum components in the vicinity of 1064 nm containing several picojoules of energy were produced by soliton self-frequency shift in a photonic crystal fiber (PCF). In this case the amount of energy contained within the Nd:YAG emission band was well below 1 pJ and ASE level at the output of amplifiers was measured to be of $\sim 2 \times 10^{-4}$ with reference to intensity of the main ~ 60 ps pulse. Employment of the pulse cleaner led to the contrast enhancement by more than two orders of magnitude (see Fig. 9b) with modest influence on the amplified pulse energy and temporal characteristics.

In the **forth** chapter the results of numerical simulations and experimental investigation of flat top picosecond pulse formation are presented. The OPCPA pump pulses with a rectangular (flat top) temporal profile and a duration comparable to that of the seed pulse would provide a uniform gain for all seed spectral components, thereby avoiding spectral gain narrowing, increasing pump-to-signal conversion efficiency [32] and improving amplified pulse contrast ratio in respect to parametric superfluorescence background [34]. Our introduced method for picosecond pulse envelope shaping is based on pulse temporal profile transformations during cascaded second harmonic generation. The main idea of the flat top pulse formation could be presented as follows. In a second harmonic generation

process the temporal profile of the fundamental harmonic (FH) pulse undergoes significant changes that are governed by the input pulse temporal profile and frequency conversion efficiency. In case of pulses with Gaussian temporal profile, the growth of energy conversion to the second harmonic (SH) leads to flattening of residual fundamental pulse envelope and consequent formation of dip in the temporal pulse profile. The modified fundamental pulse leaving the first second harmonic generator could be used as a pump pulse in the second stage of harmonic generator. In order to find out the conditions for effective pulse envelope transformations employing cascade SH generators we have performed a numerical simulation of the three-wave parametric interaction using the symmetrized split-step method [44, 45]. Numerical simulations were performed for the case of two stage cascaded SH generation employing a type-I (oo-e) phase matching DKDP crystals with a length $L=10$ mm in the first stage and $L=20$ mm in the second stage of SH generator. It was assumed that the FH pump pulse entering the SH generators have a Gaussian temporal profile with pulse width at FWHM of 70 ps. Simulation results presented in Fig. 10a reveal that changes in temporal profile of the residual FH after the first stage of SH generation when increasing pump pulse intensity I_p are quite substantial.

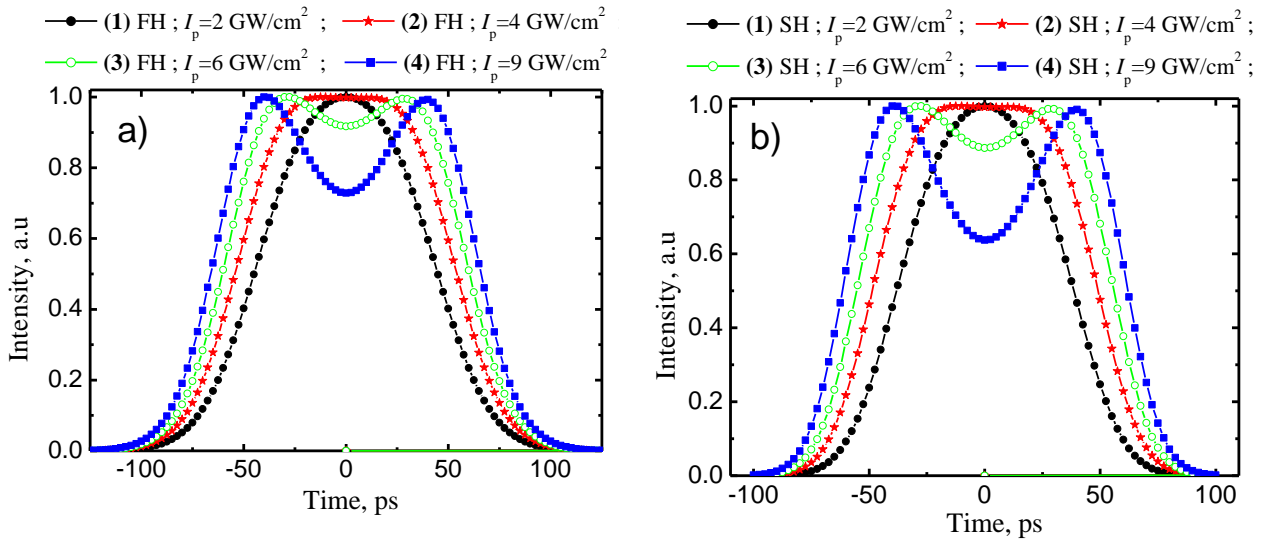


Fig. 10. Simulated pulse temporal profiles on the beam axis of: a) FH pulses after the first stage of the SH generator for different pump pulse peak intensities; b) SH pulses after the second stage of the SH generator for different pump pulse peak intensities. I_p is the pump peak intensity at the first stage of the SH generator.

At pump intensity value of $I_p=4 \text{ GW/cm}^2$ the FH pulse envelope takes flat top temporal profile exhibiting the pulse intensity plateau region of $\approx 50 \text{ ps}$ (line (2) in Fig.10a). Note, that in this case the pulse duration defined at FWHM increases up to 111 ps. Further increase of pump intensity results in progressively growing envelope modulation of the FH pulse (see lines (3), (4) in Fig.10a). In the second step we have performed the computer simulation of the SH generation using the fundamental harmonic pulses depicted in Fig.10a as a pump for the second stage of the SH generator. The simulation results, presented in Fig. 10b, shows that the temporal profile of the SH pulse generated in the second stage tends to repeat the pump pulse temporal profile with modestly reduced pulse duration and increased temporal modulation.

The experiment was carried out using Nd:YAG based amplification system developed for pumping of OPCPA (described in the sixth chapter of this thesis). In our setup, schematically presented in Fig. 11, Yb:KGW fs oscillator (Light conversion, Ltd.) which provides pulses of a 60 fs duration and 9 nJ of energy at a 78 Mhz repetition rate was used as a seed source both for femtosecond Yb:KGW regenerative amplifiers and for picosecond Nd:YAG amplification system. Nd:YAG power amplifier boosted pulses energy up to 500 mJ at repetition rate of 10 Hz. The spatial shape of the output beam had a smooth intensity distribution (see inset in Fig.11) which was well approximated by the third order hyper-Gaussian function. In experiment the DKDP crystals of 10 mm or 13 mm length were used in the first stage of SH generator, while the length of the crystal in the second stage was 20 mm. All the crystals were cut for type I phase matching at polar angle $\theta=36.6^\circ$ and azimuthal angle $\phi=45^\circ$. The measurements of the temporal shape of the FH pulses were performed by using the third-order cross-correlator (Sequoia, Amplitude Technologies) designed for 1000–1150 nm wavelength range. We have modified the arrangement of the cross-correlator for the measurements of picosecond pulse temporal profile by setting up an additional beam path for $\sim 300 \text{ fs}$ probe pulses delivered by PHAROS system.

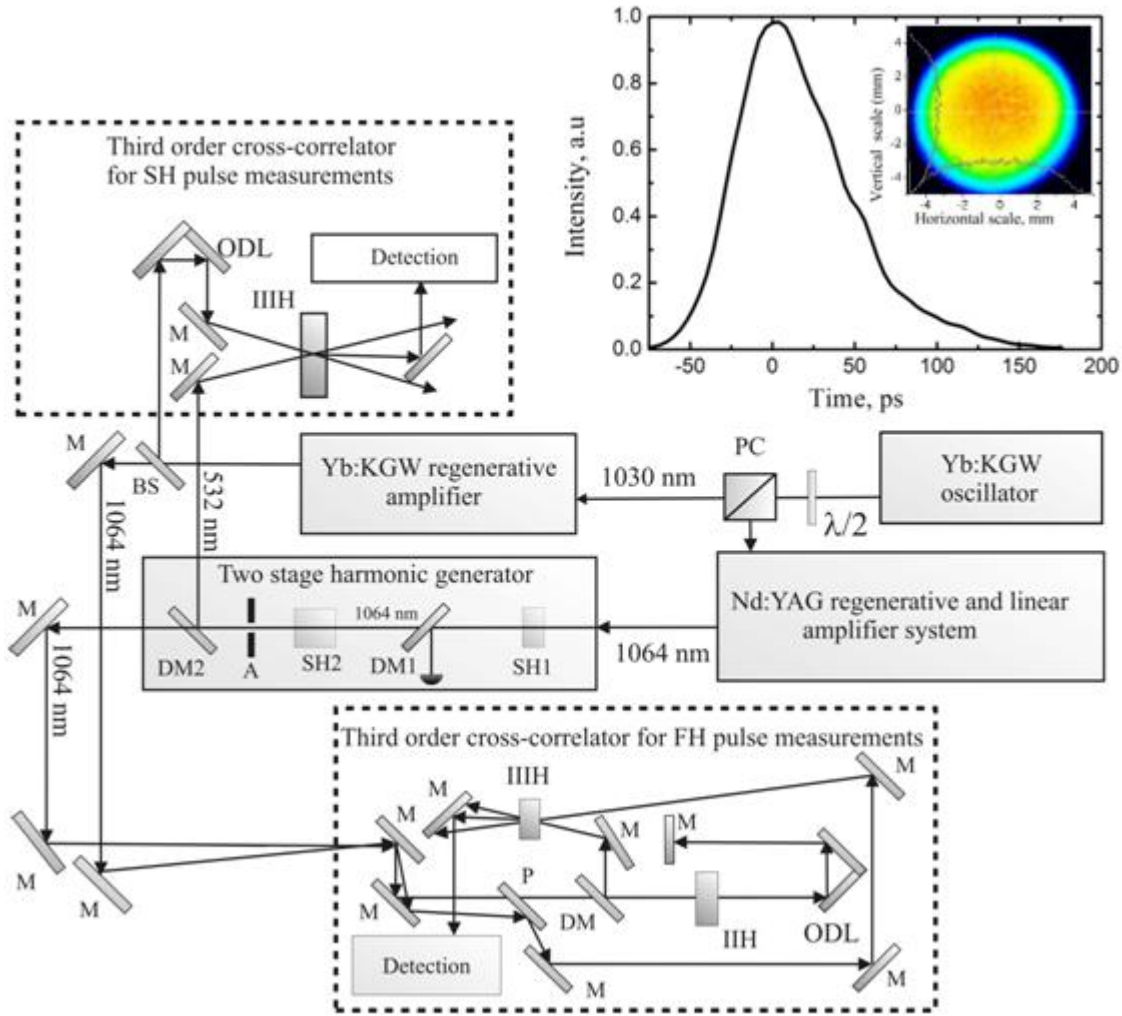


Fig.11 Picosecond pulse shaping and measurement system : M – mirrors, ODL-optical delay line, SH1 – DKDP crystal (10 or 13 mm of length), SH2 – DKDP crystal 20 mm of length, IIIH and IIIH – the second and the third harmonic crystals for the pulse cross-correlation measurements respectively, DM-dichromatic mirrors, A – aperture, PC – polarization cube. Inset shows the FH pulse temporal profile and the beam intensity spatial distribution at the output of Nd:YAG amplifiers.

In the initial experiments the pulse envelope modification taking place in the center of beam was measured. A 1.5 mm size aperture was placed in front of the beam of the FH pulses leaving the first SH generation stage in order to eliminate effects related to varying pulse intensity across the FH beam. Measured pulse temporal profiles are presented in Fig.12.

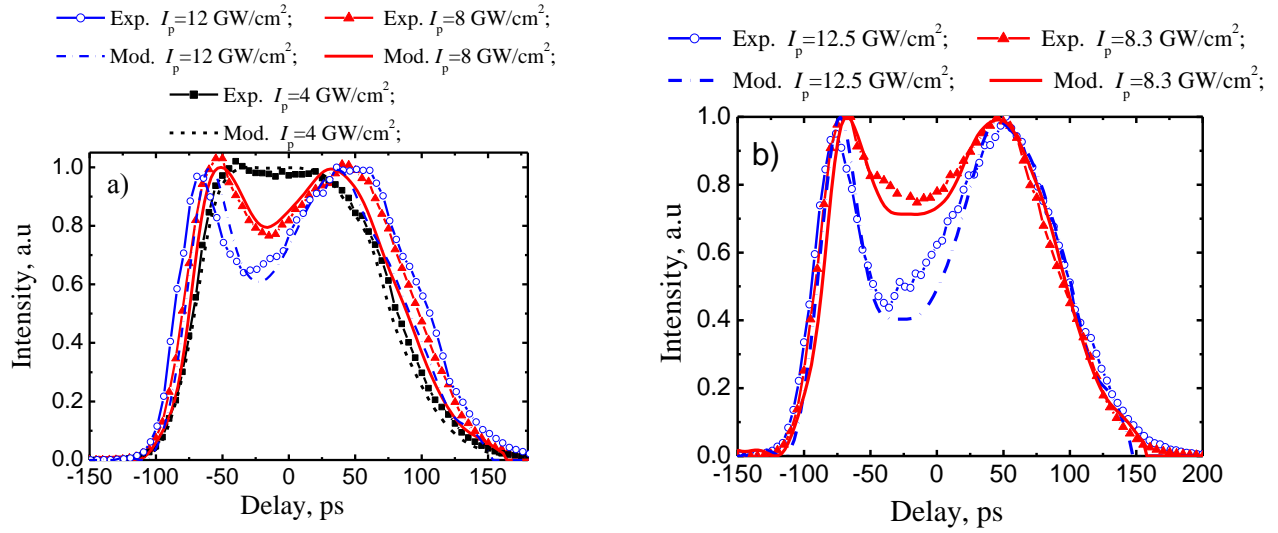


Fig. 12 The temporal profile of residual FH pulse in the beam center at different pump intensities for 10 mm (a) and 13 mm (b) long DKDP crystals. Circles, triangles and squares represents experimental data, lines shows results of numerical modeling.

The experiment confirmed expectations that due to intensity dependent three wave parametric interaction the flattening of initial bell shaped FH pulse takes place and at certain pump intensity level the pulse envelope of residual FH becomes the flat-top shaped. Further increase of pump intensity and corresponding conversion efficiency to the SH leads to appearance of a dip in the pulse temporal envelope. The measured pulse temporal profiles were in good agreement with the results of computer simulations performed using actual pump pulse characteristics.

In Fig.13 the results of flattened pulse shape measurements performed acquiring the signal from whole the beam are presented. We have shown that at the particular the second harmonic generation conditions the 1064 nm pump pulses with temporal profile close to Gaussian and pulse width of ~ 75 ps at FWHM can be converted to pulses of the fundamental and the second harmonic with hyper-Gaussian temporal profile having intensity plateau region extending over ~ 100 ps time interval.

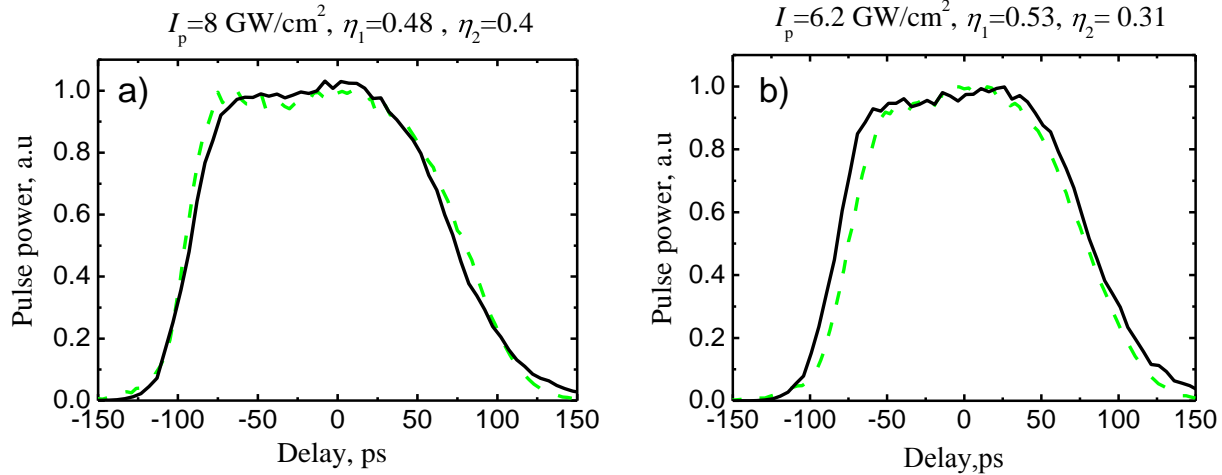


Fig. 13 Flat top pulses from cascade SH generator using 10 mm (a) and 13 mm (b) long crystals in the first SH generation stage: solid lines – temporal profile of FH pulses, dashed lines – temporal profile of SH pulses. η_1 and η_2 indicate the conversion efficiency in the first and second stage of SH generator, respectively.

The main condition for flat top pulse formation is that the energy conversion efficiency in the first stage of harmonics generator should be around 45 – 50 %. The obtained results were roughly the same for both the DKDP crystal length of 10 mm and 13 mm. The only difference was that maximum pulse temporal profile flattening for the crystal of 13 mm was recorded at ~25 % lower pump pulse energy. So, the flat top pulse can be generated using nonlinear crystal of different length and attaining 45 – 50 % pump to the SH conversion efficiency by adjusting pump pulse intensity.

Flat top the second harmonic pulses at 532 nm were obtained in the second stage of SH generator (see Fig.11). The energy conversion efficiency to the SH in 20 mm long of DKDP crystal was in the range of 20 – 40% depending on pump pulse energy. The temporal structure of the ps second harmonic pulses, generated in the second SHG stage, was characterized by the home-made third-order cross-correlator in which 1030 nm femtosecond pulses from PHAROS system were used for the 532 nm picosecond pulses probing (see Fig. 11). The SH pulse temporal profiles measured for the different FH pulse intensities I_p at the entrance of two stage SH generator are presented in Fig. 13. Similar to results of computer

simulations, in the case of flat-top pump pulses both the SH pulse duration and the width of the intensity plateau corresponds to those of the pump pulse with accuracy of $< 95 \%$.

The OPCPA output energy increases with the rise of pump pulse energy. Therefore we have examined the possibility for distortion-free amplification of flat top pulses in additional laser amplifier compensating in this way the $\sim 50 \%$ pulse energy losses taking place during second harmonic generation. The results of this experimental investigation is presented in the **fifth** chapter of this thesis. The schematic of experimental set-up is presented in Fig.14. In case of pulses with Gaussian temporal profile (1) the growth of energy conversion to second harmonic (SH) leads to flattening of residual fundamental pulse envelope (2) and even to formation of dip in the temporal pulse profile. The modified fundamental pulse leaving the first second harmonic generator could be amplified and used as a pump pulse in the second stage of harmonic generators (SH2). The SH generator pumped by amplified flat top pulses (3) will produce flat top pulses of second harmonic as well (4). The main goal of the experiment was to clarify to which extent the amplification saturation effect distorts the temporal profile of amplified pulses.

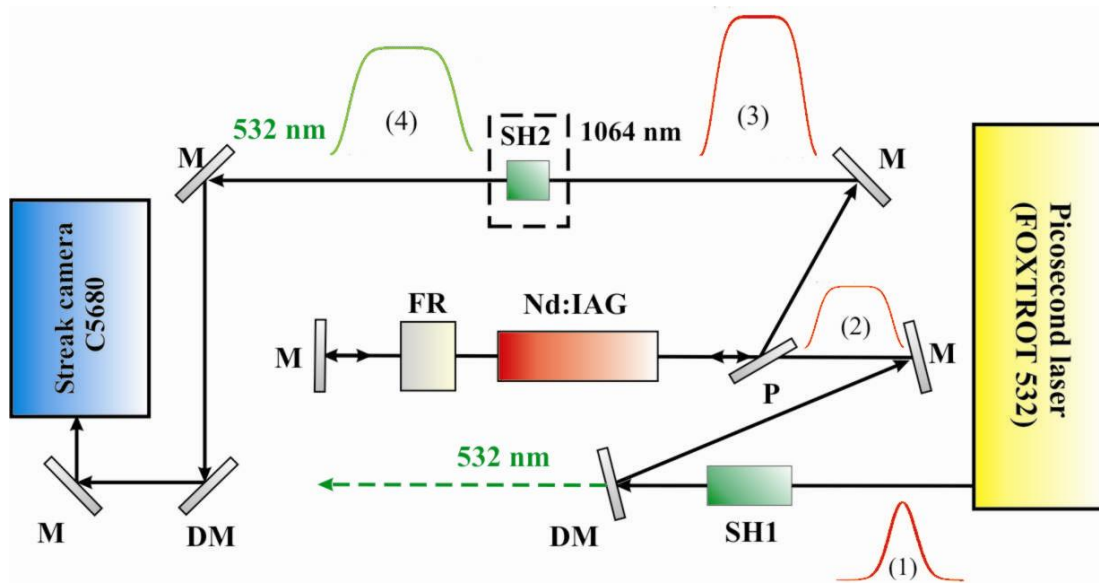


Fig. 14 Picosecond pulse shaping – amplification system: SH1 and SH2 – second harmonic crystals, FR – Faraday rotator, M – mirrors, DM – Dichromatic mirrors, P – polarizer.

The experimental results are presented in Fig.15. The experiment was carried out by pumping 10 mm of length LBO crystal (SH1) with 56 ps width (at FWHM) and 0.4 mJ of energy Gaussian pulses (line (1) in Fig. 15). Pulses having an intensity plateau region extending 50 ps time interval were formed (line (2)) when conversion efficiency in the SH1 was around 50 %. Shaped pulses were amplified in the double pass power amplifier up to 1.7 mJ of energy what corresponds to pulse intensity of $I_{0,5}=1.28 \text{ GW/cm}^2$ and energy fluence of $F_{0,5}=0.128 \text{ J/cm}^2$. Then pulses were frequency doubled in the 3 mm length KTP crystal (SH2), Pulse profiles were measured with streak camera C5680 (Hamamatsu Photonics).

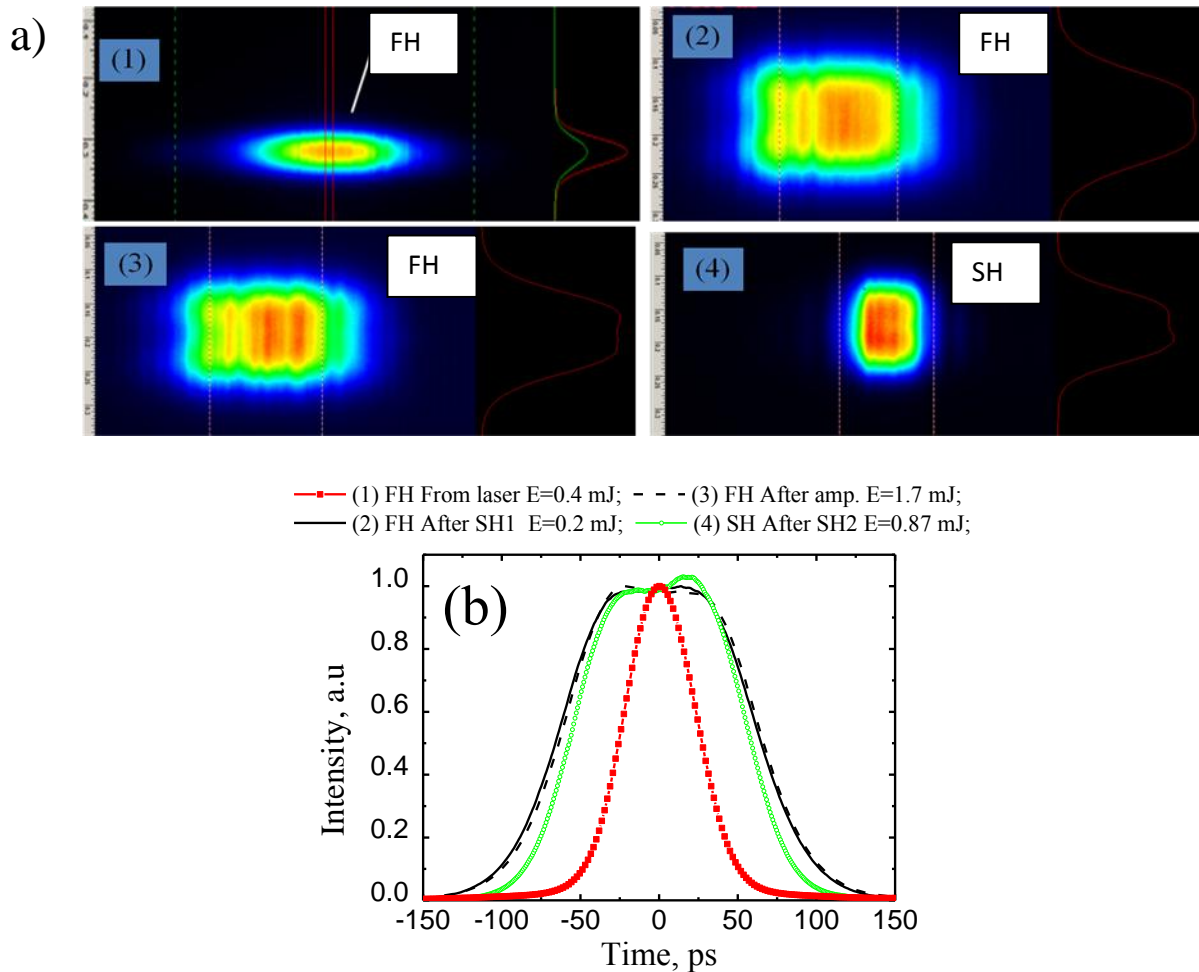


Fig. 15 Picosecond pulse temporal profiles after subsequent pulse shaping-amplification stages.: a) Streak camera view ; b) Data extracted from streak camera view.

The results of the measurements presented in Fig.15 indicate that in our experimental conditions the changes in temporal profile during amplification are less than 2% (see lines 2 and 3). In the **sixth** chapter of this thesis we overview final multi-milijoule system for OPCPA pump. This system comprises the tandem diode pumped Nd:YAG regenerative amplifier (see Fig. 16) and flash lamp pumped Nd:YAG power amplifier.

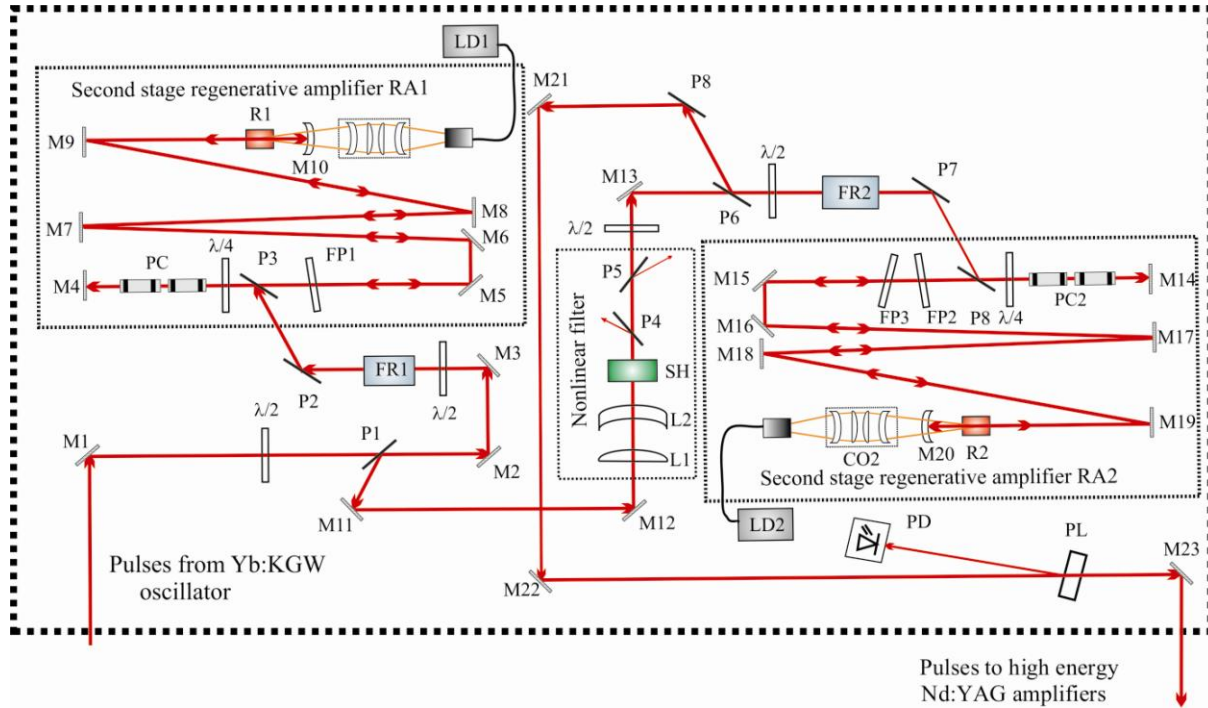


Fig. 16 Schematic of Nd:YAG regenerative amplifier system. M1-M23 – mirrors; L1,L2 – lenses; PC1, PC2– Pockels cell; FP1-FP3 – Fabry-Perot interferometers; LD1, LD2 – pump laser diodes; PL – glass plate, PD – detector, CO1,CO2 – coupling optics, R1, R2 – Nd:YAG rod, P1-P8 – polarizers. SH – second harmonic crystal.

The key feature of our system is the direct seeding of Nd:YAG amplifiers with femtosecond pulses of a Yb:KGW oscillator which is simultaneously used to pump and seed an optical parametric amplifier (OPA). Such an approach ensures reliable all-optical pump – signal synchronization in OPCPA system stages. In our setup (see Fig. 17), the femtosecond Yb:KGW oscillator (Light conversion Ltd., Lithuania) which generates 60-fs, 9-nJ pulses at a 78-MHz repetition rate was used as a seed source. A part of the oscillator output was coupled into the Nd:YAG amplification system, remainder of the pulse was used as a seed for the femtosecond Yb:KGW amplifier (Fig. 17). High-order half-wave plate and polarization cube were used as a spectrally selective beam splitter. The Yb:KGW and

Nd:YAG amplifiers operated at different wavelengths, namely 1030 nm and 1064 nm. To realize a spectrally selective polarization beam splitter, the phase retardation quartz plate of special design was fabricated inducing a phase shift of 2π at 1064 nm and of π at 1030 nm. As a result, the spectral component at 1030 nm changed the polarization state into orthogonal and was coupled into the Yb:KGW RA.

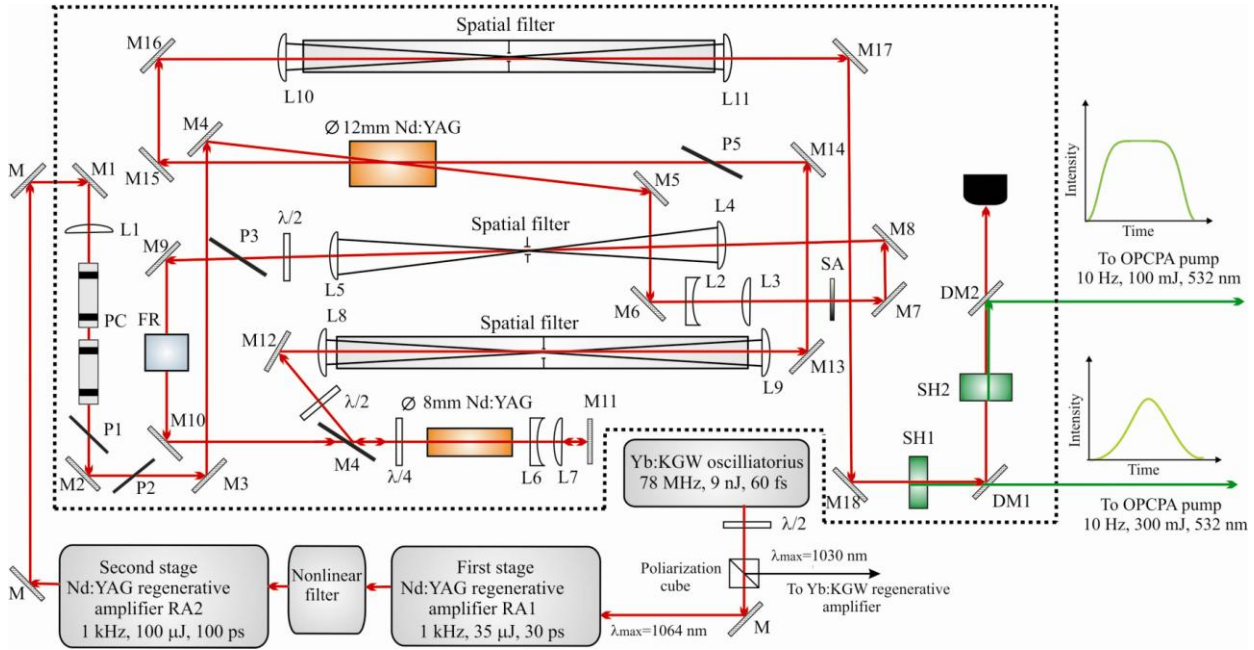


Fig. 17 Schematic of the whole Nd:YAG amplification system for OPCPA pump: SA serrated aperture; SH1 and SH2 second harmonic crystal; M1 – M18 mirrors, L1-L11 lenses, P1-P5 polarizers, DM1-DM2 – dichromatic mirrors, FR – Faraday rotator, PC – Pockels cell .

The spectral component, which preserved its polarization state at 1064 nm, was coupled into the Nd:YAG regenerative amplifier system. The estimated seed energy within the fluorescence bandwidth of the Nd:YAG centered at 1064 nm was 12 pJ. The 1-kHz repetition rate RA1 was based on the Nd:YAG rod ($\varnothing 6 \times 10$ mm) pumped by a 3 W cw laser diode. The maximum amplified pulse energy of 45 μ J was limited by the Kerr effect and resistance to radiation damage of the Nd:YAG rod coating. The amplified pulse intensity contrast was 4×10^{-7} . For further pulse amplification up to 100 μ J and pulse temporal intensity profile formation in multiple intra-cavity etalon system (discussed in the second chapter) we used the second stage regenerative amplifier (RA2), pumped by 4.5 W cw laser diode. The pulse contrast at the RA2 output was at level of $\sim 3 \times 10^{-6}$. After implementation

of our develop nonlinear filter (see the third chapter), pulse contrast ratio was improved up to 1.5×10^{-8} . In the flash lamp pumped Nd:YAG power amplifier (Fig. 17) spatial characteristics of the pump beam was carefully tailored. The pump beam profile is one of the critical issues in high energy OPCPA system development. First of all, the spatial beam profile should be uniform to ensure uniform intensity distribution of the amplified signal beam profile. Furthermore, the beam profile must provide maximal extraction of the energy stored in active elements (AEs) at a safe level of the output peak intensity. On the other hand, when the beam cross section significantly exceeds the AE cross section, diffraction from the AE edges can initiate small-scale self-focusing and lead to AE damage. It is shown [46] that the top-hat beam profile (hyper-Gaussian beam distribution) is the best solution to the above requirements. We have designed a beam shaping system using a serrated pattern aperture (SA in Fig 17) followed by an imaging spatial filter. The plane of the aperture was relay imaged to the entrance plane of the rod AE of the amplification stage (\varnothing 8 mm). The diameter d_{ap} of the spatial filter aperture was chosen following criteria $d_{ap} \leq f\lambda/2L$ [47] where f is the focal length of the first lens of the filter, L is the serration period of the aperture. The chosen aperture diameter of 0.6 mm was about five times smaller than upper limit obtained from presented criteria evaluation formula.

Beam profiles after the aperture and in the relay imaged plane are given in Fig.18. Before forming the spatial profile, a 100 ps pulse beam from the RA2 output passed through the \varnothing 12 mm amplifier rod at a small angle to the rod axis for 10 fold pre-amplification. The Gaussian output of RA2 using the beam shaping system was transformed to an approximately second-order hyper-Gaussian beam (Fig. 18b). During amplification, the beam profile due to gain saturation and nonuniform amplification in the AE becomes more flattened. The final spatial beam profile after \varnothing 8 mm and \varnothing 12 mm amplification stages can be approximated by the third-order hyper-Gaussian distribution (Fig. 18c). The amplified 600 mJ pulse was frequency doubled in a second harmonic DKDP crystal with 50 % efficiency. The second harmonic crystal was placed in the relay image plane of the output of the \varnothing 12 mm amplifier stage. The second harmonic beam profile at a distance of 1.5 m from the nonlinear crystal still shows no diffraction rings (Fig. 19b), but exhibits

some asymmetry (ellipticity factor ~ 0.7). The residual radiation of the fundamental harmonic after SH generation in the first stage is effectively used in the second SH generation stage (Fig. 17) for the formation of pump pulses with sufficiently broad intensity plateau region (~ 100 ps). The use of such pulses as a pump for high gain OPCPA system stages minimize the effect of seed pulse spectrum narrowing and allows to reduce energy of parametric superfluorescence signal which deteriorate the final pulse contrast.

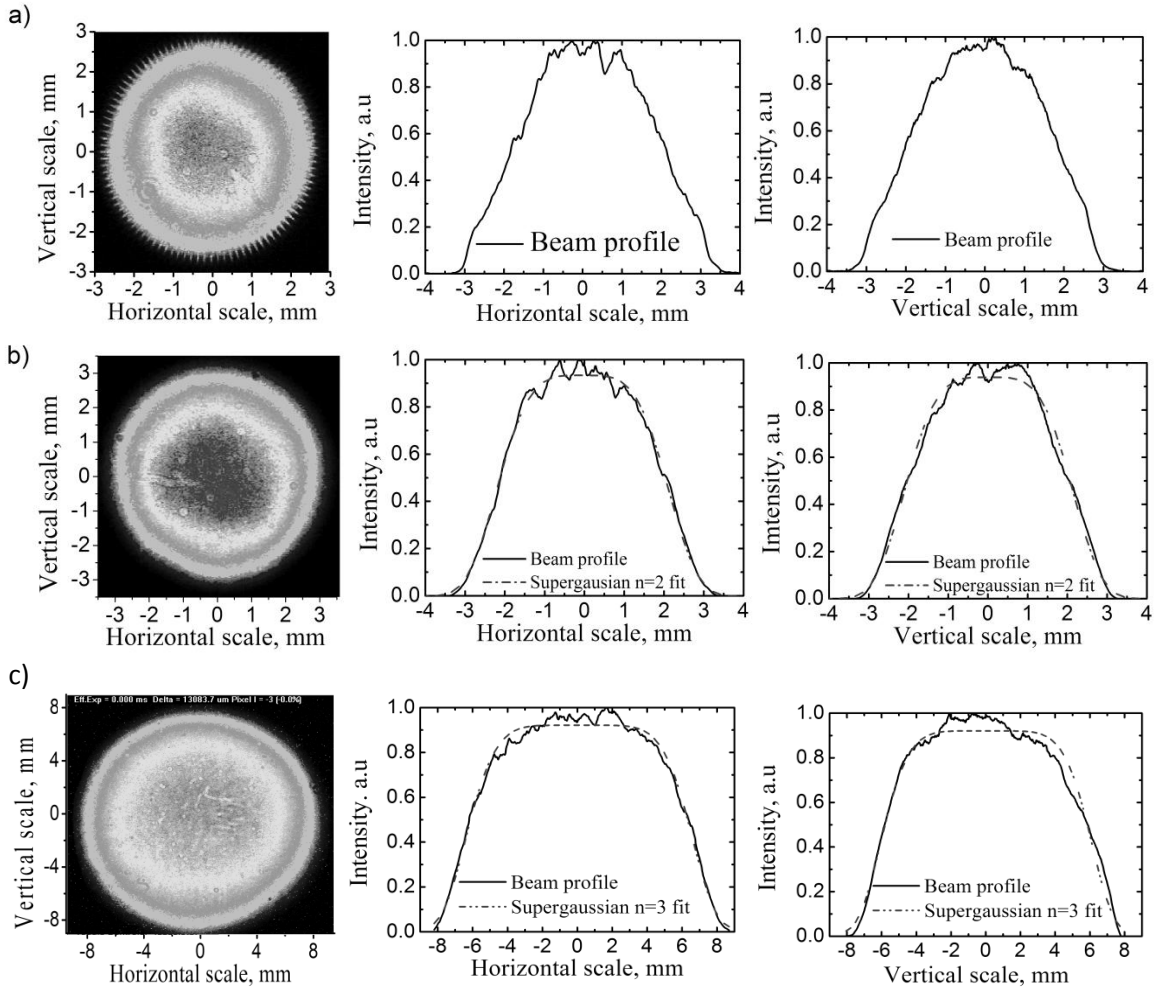


Fig. 18. Spatial beam intensity distributions at a distance of 10 cm behind the serrated aperture (a), at the input of the Nd:YAG AE of the $\varnothing 8$ mm (b) and at the output of the amplification stage $\varnothing 12$ mm (c). The pulse energy is 600 mJ. Solid lines show the spatial profile, dashed curves is the approximation by the second-order (b) and third-order (c) hyper-Gaussian function.

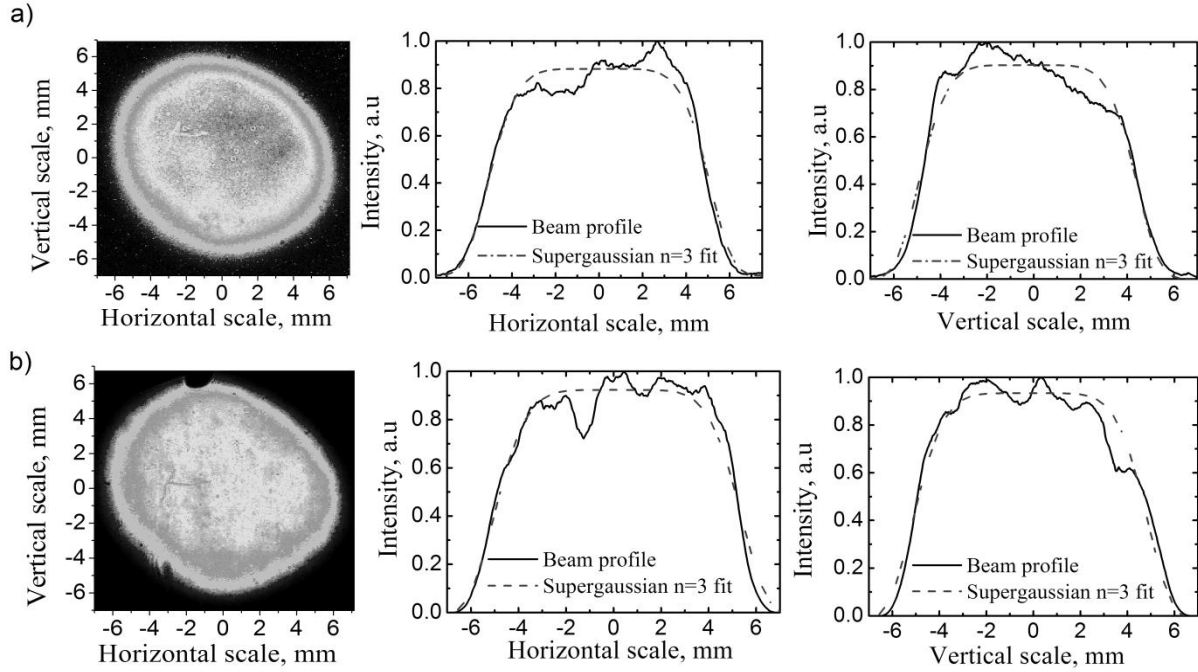


Fig. 19. Spatial beam intensity distributions at a distance of 150 cm from the SH crystal for the fundamental beam profile (a) and SH beam profile (b). Solid lines show the spatial profile, dashed curves is the approximation by the third-order hyper-Gaussian function.

The SH pulse generated in the first stage retains Gaussian temporal profile, but still can be efficiently applied as a pump in the last stage of a multi-stage OPCPA setup. This stage usually is operated in the regime of small gain and strong saturation [46] what allows to avoid the amplified pulse spectrum narrowing caused by Gaussian temporal profile of pump pulses.

Main results and conclusions

1. Formation of picosecond pulses in Nd:YAG regenerative amplifiers employing two intracavity Fabry-Perot interferometers and the ~ 60 fs pulses seed from Yb:KGW oscillator has been investigated. It was shown by computer simulations that modulation of picosecond pulse envelope can be minimized by inserting a second intra-cavity Fabry-Perot etalon with the optimal base which is equal to half the thickness of the first one.
2. The amplification ratio of 10^7 in two stage regenerative amplifier with intracavity etalons and formation of smooth envelope ~ 100 ps pulses has been demonstrated experimentally.
3. The picosecond pulse temporal contrast enhancement by use of the second-order nonlinearity-dependent fundamental pulse polarization rotation in unbalanced phase second harmonic generators has been demonstrated for the first time. The contrast enhancement factor of 140 for the < 1 GW/cm² intensity picosecond pulses using type-II phase-matching KTP crystal has been achieved.
4. It was shown that the employment of nonlinear intensity dependent filter in between of regenerative amplification stages provides amplified pulse contrast enhancement without losses in output pulse energy. The ASE intensity at the output of Nd:YAG regenerative amplifier seeded by ~ 10 pJ from Yb:KGW oscillator has been reduced from 3×10^{-6} down to 1.5×10^{-8} level. When $\sim 0,1$ pJ energy Ti:sapphire oscillator pulses, transmitted by photonic crystal, were used as a seed, the ASE intensity level at the output of amplifier was lowered from 2×10^{-4} to 10^{-6} .
5. It was shown that operating DKDP crystal based second harmonic generator at 45–50 % energy conversion conditions the ~ 75 ps FWHM fundamental pulses with temporal profile close to Gaussian can be converted to pulses with hyper-Gaussian profile pulses having intensity plateau region extending over ~ 100 ps time interval. Further increase of conversion efficiency to the SH leads to appearance of a dip in the pulse temporal envelope. The similar trends in the pulse envelope transformations has been observed when generating SH in the LBO crystal pumped by 56 ps pulses.

6. The flat top pulses at 532 nm were obtained in the second stage of SH generator pumped by hyper-Gaussian 1064 nm pulses generated in the first SH generation stage. Both the SH pulse duration and the width of the intensity plateau corresponds to those of the pump pulse with accuracy of 95 % when energy conversion in second SH stage is above 30%. The use of flat top pulses for the pumping of OPCPA systems allows to gain more benefits of this amplification method.
7. It was shown that amplifying flat top pulses in the two pass diode pumped Nd:YAG amplifier characterized by amplification ratio of 8, output pulse intensity of $I_{0,5}=1,3 \text{ GW/cm}^2$ and output fluence of $F_{0,5}=0.128 \text{ J/cm}^2$ the changes in the temporal amplified pulse profile are negligible.
8. The relatively high output energy system of Nd:YAG amplifiers for pumping of OPCPA systems has been developed. It is optically synchronized with pulses of Yb:KGW oscillator and features two 532 nm outputs with pulse parameters: a) Gaussian pulse profile, ~ 300 mJ energy, 75 ps pulse width; b) hyper-Gaussian pulse profile, ~100 mJ energy, pulse width 100-150 ps.

Reference list

- [1] W. E. Lamb, Theory of an optical laser, *Phys. Rev.* **134** (6A), A1429-A1450 (1964).
- [2] L. E. Hargrove, R. L. Fork, and M. A. Pollack, Locking of He–Ne laser modes induced by synchronous intracavity modulation, *Appl. Phys. Lett.* **5**(1), 4-5 (1964).
- [3] E. Goulielmakis, M. Schultze, M. Hofstetter, V. S. Yakovlev, J. Gagnon, M. Uiberacker, A. L. Aquila, E. M. Gullikson, D. T. Attwood, R. Kienberger, F. Krausz, and U. Kleineberg, Single-Cycle Nonlinear Optics, *Science* **320**(5883), 1614-1617 (2008).
- [4] C. J. Bardeen, Q. Wang, C. V. Shank, Selective Excitation of Vibrational Wave Packet Motion Using Chirped Pulses, *Phys. Rev. Lett.* **75**(19), 3410-3413 (1995).
- [5] B. Kohler, V.V. Yakovlev, J. Che, J.L. Krause, M. Messina, K.R. Wilson, N. Schwentner, R.M. Whitnell, Y. Yan, Quantum Control of Wave Packet Evolution with Tailored Femtosecond Pulses, *Phys. Rev. Lett.* **74**(17), 3360-3363 (1995).
- [6] A. H. Zewail, Femtochemistry: Recent Progress in Studies of Dynamics and Control of Reactions and Their Transition States, *J. Phys. Chem.* **100**(31), 12701-12724 (1996).
- [7] T. Brabec and F. Krausz, Intense few-cycle laser fields: Frontiers of nonlinear optics, *Rev. Mod. Phys.* **72**(2), 545-591 (2000).
- [8] M. Drescher, M. Hentschel, R. Kienberger, G. Tempea, C. Spielmann, G. A. Reider, P. B. Corkum, and F. Krausz, X-ray pulses approaching the attosecond frontier, *Science* **291**(5510), 1923–1927 (2001).
- [9] E. Goulielmakis, M. Schultze, M. Hofstetter, V. S. Yakovlev, J. Gagnon, M. Uiberacker, A. L. Aquila, E. M. Gullikson, D. T. Attwood, R. Kienberger, F. Krausz and U. Kleineberg, Single-cycle nonlinear optics, *Science* **320** (5883), 1614–1617 (2008).
- [10] D. Strickland and G. Morou, Compression of amplified chirped optical pulses, *Opt. Commun.* **56** (3), 219–221 (1985).
- [11] C. P. J. Barty, T. Guo, C. Le Blanc, F. Raksi, C. R. Petrucci, J. Squier, K. R. Wilson, V. Yakovlev, K. Yamakawa, Generation of 18-fs, multiterawatt pulses by regenerative pulse shaping and chirped-pulse amplification, *Opt. Lett.* **21**(9), 668-670 (1996).
- [12] S. A. Akhmanov and R. V. Khokhlov, Concerning one possibility of amplification of light waves, *Sov. Phys. JETP* **16**, 252-257 (1963).
- [13] S. A. Akhmanov, V. V. Fadeev, R. V. Khokhlov, A. I. Kovrigin, A. P. Piskarskas, Observation of parametric amplification in the optical range, *JETP Lett.* **2**, 191-193 (1965).

- [14] A. Dubietis, G. Jonušauskas, A. P. Piskarskas, Powerful femtosecond pulse generation by chirped and stretched pulse parametric amplification in BBO crystal, *Opt. Commun.* **88**(4-6), 437-440 (1992).
- [15] A. Dubietis, R. Butkus and A. P. Piskarskas, Trends in chirped pulse optical parametric amplification, *IEEE J. Sel. Top. Quantum Electron.* **12** (2), 163-172 (2006).
- [16] S. Adachi, N. Ishii, T. Kanai, A. Kosuge, J. Itatani, Y. Kobayashi, D. Yoshitomi, K. Torizuka and S. Watanabe, 5-fs, multi-mJ, CEP-locked parametric chirped-pulse amplifier pumped by a 450-nm source at 1 kHz, *Optics express* **16** (19), 14341-14352 (2008).
- [17] J. Rothhardt, S. Hädrich, E. Seise, M. Krebs, F. Tavella, A. Willner, H. Schlarb, J. Feldhaus, J. Limpert, J. Rossbach, A. Tünnermann, High average and peak power few-cycle laser pulses delivered by fiber pumped OPCPA system, *Opt. Express* **18** (12), 12719-12726 (2010).
- [18] A. H. Curtis, B. A. Reagan, K. A. Wernsing, F. J. Furch, B. M. Luther, and J. J. Rocca, Demonstration of a compact 100 Hz, 0.1 J, diode-pumped picosecond laser, *Opt. Lett.* **36** (11), 2164-2166 (2011).
- [19] B. A. Reagan, A. H. Curtis, K. A. Wernsing, F. J. Furch, B. M. Luther and J. J. Rocca, Development of high energy diode-pumped thick-disk Yb:YAG Chirped-Pulse Amplification lasers, *IEEE J Quantum Electronics* **48** (6), 827-835 (2012).
- [20] S. Witte, R. T. Zinkstok, W. Hogervorst, and K. S. E. Eikema, Generation of few-cycle terawatt light pulses using optical parametric chirped pulse amplification, *Opt. Express* **13**, 4903-4908 (2005).
- [21] D. Herrmann, L. Veisz, R. Tautz, F. Tavella, K. Schmid, V. Pervak, and F. Krausz, Generation of sub-three-cycle, 16 TW light pulses by using noncollinear optical parametric chirped-pulse amplification, *Opt. Lett.* **34**, 2459-2461 (2009).
- [22] V. V. Lozhkarev, G. I. Freidman, V. N. Ginzburg, E. V. Katin, E. A. Khazanov, A. V. Kirsanov, G. A. Luchinin, A. N. Mal'shakov, M. A. Martyanov, O. V. Palashov, A. K. Poteomkin, A. M. Sergeev, A. A. Shaykin and I. V. Yakovlev, Compact 0.56 petawatt laser system based on optical parametric chirped pulse amplification in KD*P crystals, *Laser Phys. Lett.* **4**(6), 421-427 (2007).
- [23] O. Chekhlov, E. J. Divall, K. Ertel, S. J. Hawkes, C. J. Hooker, I. N. Ross, P. Matousek, C. Hernandez-Gomez, I. Musgrave, Y. Tang, T. Winstone, D. Neely, R. Clarke, P. Foster, S. J. Hancock, B. E. Wyborn and J. L. Collier, Development of petawatt laser amplification systems at the Central Laser Facility, *Proc. SPIE* **6735**, 67350J (2007).
- [24] M. Hemmer, A. Vaupel, M. Wohlmuth, M. Richardson, OPCPA pump laser based on a regenerative amplifier with Bragg grating spectral filtering, *Appl. Phys. B* **106** (3), 599-603 (2012).
- [25] N. Ishii, C. Y. Teisset, T. Fuji, A. Baltuška, F. Krausz, Seeding of an eleven femtosecond amplifier and its Nd picosecond pump laser from a single broadband Ti:sapphire oscillator, *IEEE J. Quantum Electron.* **12**(2), 173-180 (2006).

- [26] H. Zeng, J. Wu, H. Xu, K. Wu, E. Wu, Generation of accurately synchronized pump source for optical parametric chirped pulse amplification, *Appl. Phys. B* **79**, 837-839 (2004).
- [27] C. Y. Teisset, N. Ishii, T. Fuji, T. Metzger, S. Köhler, R. Holzwarth, A. Baltuška, A. M. Zheltikov and F. Krausz, Soliton-based pump-seed synchronization for few-cycle OPCPA, *Opt. Express* **13** (17), 6550-6557 (2005).
- [28] D. Yoshitomi, X. Zhou, Y. Kobayashi, H. Takada, and K. Torizuka, Long-term stable passive synchronization of 50 μ J femtosecond Yb-doped fiber chirped-pulse amplifier with a mode-locked Ti:sapphire laser, *Optics Express* **18**(25), 26027-26036 (2010).
- [29] H. Tsuchida, Pulse timing stabilization of a mode-locked Cr:LiSAF laser, *Opt. Lett.*, **24**, 1641–1643 (1999).
- [30] O. D. Mücke, D. Sidorov, P. Dombi, A. Pugžlys, S. Ališauskas, V. Smilgevičius, N. Forget, J. Pocius, L. Giniūnas, R. Danielius, and A. Baltuška, 10-mJ Optically Synchronized CEP-Stable Chirped Parametric Amplifier at 1.5 μ m, *Optics and Spectroscopy*, **108** (3), 456–462 (2010).
- [31] G. Andriukaitis, T. Balčiūnas, S. Ališauskas, A. Pugžlys, A. Baltuška, T. Popmintchev, M. C. Chen, M. M. Murnane, and H. C. Kapteyn, 290 GW peak power few-cycle mid-infrared pulses from an optical parametric amplifier, *Opt. Lett.* **36**(15), 2755-2757 (2011).
- [32] L. J. Waxer, V. Bagnoud, I. A. Begishev, M. J. Guardalben, J. Puth, J. D. Zuegel, High-conversion-efficiency optical parametric chirped-pulse amplification system using spatiotemporally shaped pump pulses, *Opt. Lett.* **28**, 1245-1247 (2003).
- [33] G. Cerullo and S. De Silvestri, Ultrafast optical parametric amplifiers, *Rev. Sci. Instrum.* **74**, 1-18 (2003).
- [34] S. Witte and K. S. E. Eikema, Ultrafast Optical Parametric Chirped-Pulse Amplification, *IEEE J. Quantum Electron.*, **18**(1), 296-307 (2012).
- [35] J. Moses, C. Manzoni, S. W. Huang, G. Cerullo and F. X. Kaertner, Temporal optimization of ultrabroadband high-energy OPCPA, *Opt. Express* **17**, 5540–5555 (2009).
- [36] J. A. Fulop, Z. Major, B. Horvath, F. Tavella, A. Baltuska, F. Krausz, Shaping of picosecond pulses for pumping optical parametric amplifier, *Appl. Phys. B* **87**, 79-84 (2007).
- [37] I. N. Ross, P. Matousek, G. H. C. New, K. Osvay, Analysis and optimization of optical parametric chirped pulse amplification, *J. Opt. Soc. Am. B.* **19**, (2002).
- [38] M. D. Skeldon and S. T. Bui, Temporal mode structure of a regenerative amplifier with intracavity etalons, *J. Opt. Soc. Am. B* **10**(4), 677-683 (1993).

- [39] L. Lefort, A. Barthelemy, Intensity-dependent polarization rotation associated with type II phase-matched second-harmonic generation: application to self-induced transparency, *Opt. Lett.* **20**(17), 1749-1751 (1995).
- [40] L. Leford, A. Barthelemy, All-optical transistor action by polarisation rotation during type II phase-matched second harmonic generation, *Electron. Lett.* **31**(11), 910-911 (1995).
- [41] S. Louis, V. Couderc, F. Louradour, P. Faugeras, A. Barthelemy, Nonlinear polarization evolution in type I and type II second-harmonic-generation crystals applied to the mode locking of a pulsed Nd:YAG laser *J. Opt. A: Pure Appl. Opt.* **3**(2), 139-143 (2001).
- [42] F. Louradour, A. Mugnier, A. Albert, V. Couderc, A. Barthelemy, Numerical study of quadratic polarization switching mode locking applied to femtosecond pulse generation, *Optics Commun.* **188**(5-6), 333-344 (2001).
- [43] J. Yu, Quasistationary pulse generation in flash-lamp-pumped Nd³⁺:Y₃Al₅O₁₂ laser mode locked through quadratic polarization switching, *Appl. Phys. Lett.* **89**(18), 1871- 18773 (2006).
- [44] G. Arisholm, General numerical methods for simulating second-order nonlinear interactions in birefringent media, *J. Opt. Soc. Am. B* **14**(10), 2543-2549 (1997).
- [45] S. Witte, R. Zinkstok, W. Hogervorst, and K. Eikema, Numerical simulations for performance optimization of a few-cycle terawatt NOPCPA system, *Appl. Phys. B* **87**(4), 677-684 (2007).
- [46] V. Bagnoud, I. A. Begishev, M. J. Guardalben, J. Puth, J. D. Zuegel, 5 Hz, >250 mJ optical parametric chirped-pulse amplifier at 1053 nm, *Opt. Lett.* **30**(14), 1843-1845 (2005).
- [47] J. M. Auerbach and V. P. Karpenko, Serrated-aperture apodizers for high-energy laser systems, *Appl. Opt.* **33**(15), 3178-3183 (1994).

Santrauka

DIDELĖS GALIOS PIKOSEKUNDINIS Nd:YAG LAZERIS ČIRPUOTŲ IMPULSŲ PARAMETRINIŲ STIPRINTUVŲ KAUPINIMUI

Šios disertacijos tikslas – sukurti, iširti ir optimizuoti didelės galios Nd:YAG lazerinę sistemą efektyviam moduliotos fazės signalų optinių parametrinių stiprintuvų kaupinimui.

Disertaciją sudaro įvadas, šeši pagrindiniai skyriai, rezultatų apibendrinimas ir išvados.

Įvade trumpai išdėstoma darbo motyvacija, nurodomas darbo tikslas bei uždaviniai. Pristatomas darbo naujumas, praktinė nauda, ginamieji teiginiai bei rezultatų aprobacija.

Pirmajame skyriuje apžvelgiami mokslinėse laboratorijose naudojami lazeriai, skirti čirpuotų impulsų parametrinių stiprintuvų kaupinimui. Daug dėmesio skiriama galimiems kaupinimo lazerių (stiprintuvų) ir ultratrumpųjų impulsų osciliatorių sinchronizacijos būdams. Nagrinėjama, kokie kaupinimo lazerių išvadinių impulsų spektriniai, energiniai ir laikiniai parametrai užtikrina efektyvų keleto optinių ciklų moduliotos fazės impulsų parametrinį stiprinimą.

Antrajame skyriuje pristatomi kuriamos lazerinės sistemos pikosekundinių impulsų trukmės formavimo daugelio praėjimų Fabri-Pero etalonų sistemoje eksperimentiniai ir skaitmeninio modeliavimo tyrimai. Parodėme, kad Fabri-Pero etalonų panaudojimas Nd:YAG dvipakopio regeneracinio stiprintuvo rezonatoriuose leidžia stiprinamų Yb:KGW osciliatoriaus impulsų trukmę padidinti nuo 60 fs iki 100 ps. Nustatėme, kad Nd:YAG stiprintuvų išvadinių impulsų laikinės plėtros mastas ir formuojamo impulso gaubtinės moduliacijos gylis gali būti valdomas keičiant etalonų atspindžio koeficientą. Suformuoto impulso gaubtinės moduliacijos vertė yra mažiausia, kai etalonų storio santykis artimas 2.

Trečiajame skyriuje charakterizuojamas Yb:KGW osciliatoriaus impulsus stiprinančios Nd:YAG lazerinės sistemos išvadinių impulsų kontrastas sustiprintos savaiminės emisijos (ASE) atžvilgiu. Matavimų rezultatai rodo, kad dviejų pakopų

Nd:YAG regeneracinėje sistemoje sustiprinus Yb:KGW osciliatoriaus impulsus nuo 12 pJ iki 100 μJ energijos, ASE intensyvumas išvadinėje spinduliuotėje yra 3×10^{-6} lygio smailinio impulso intensyvumo atžvilgiu. Kad būtų dar labiau pagerintas Nd:YAG lazerinėje sistemoje stiprinamų impulsų kontrastas, pritaikėme netiesinį antros eilės filtrą, veikiantį fundamentinės spinduliuotės sukimo išderintame antrosios harmonikos generatoriuje efekto pagrindu. Eksperimentiškai parodėme, kad naudojant II-sąveikos tipo KTP kristalą $< 1 \text{ GW/cm}^2$ intensyvumo impulso kontrasto gerinimo faktorius gali siekti 140 kartų. Netiesinį intensyvumų filtrą įdėję tarp regeneracinio stiprintuvo pakopų, ASE intensyvumo lygį sumažinome iki $1,5 \times 10^{-8}$ neprarasdami išvadinių impulsų energijos. Netiesinį filtrą taip pat pritaikėme ir dvipakopėje Nd:YAG regeneracinių stiprintuvų sistemoje, stiprinančioje Ti:safyro osciliatoriaus impulsus, prasklidusius fotoninių kristalų šviesolaidį. Šios Nd:YAG stiprinimo sistemos išvadinių impulsų ASE intensyvumas buvo sumažintas nuo 2×10^{-4} iki 10^{-6} .

Ketvirtajame disertacijos skyriuje pristatomi teoriniai ir eksperimentiniai duomenys, pagrindžiantys ir apibendrinantys potencialią galimybę naudojant dvipakopį antrosios harmonikos generatorių formuoti plokščios viršūnės 532 nm bangos ilgio impulsus, skirtus efektyviau parametriškai stiprinti plataus spektro impulsus su tiesine fazės moduliacija. Pristatomas pikosekundinių impulsų formavimo būdas, pagrįstas impulso laikinės formos kitimu vykstant antrosios harmonikos generacijai. Eksperimentiškai ir teoriškai parodoma, kad 45–50 % energiniu efektyvumu generuojant antrąją harmoniką DKDP kristale, 1064 nm bangos ilgio ir 75 ps trukmės Gauso laikinės formos impulsai tribangės sąveikos metu transformuojasi į hipergausinės formos laikinio profilio impulsus, kurių plokščios viršūnės sritis viršija 100 ps trukmės intervalą. Suformuotais plokščios viršūnės pirmosios harmonikos impulsais kaupiname antros pakopos harmonikų generatorių. Ištyrėme, kad išvadinio antrosios harmonikos impulso trukmė ir plokščios viršūnės sritis atitinka kaupinimo impulso formą 95 % tikslumu, kai keitimas į antrąją harmoniką antroje pakopoje viršija 30 %.

Penktajame skyriuje pristatomi pakopiniuose antrosios harmonikos generatoriuose suformuotų plokščios gaubtinės impulsų stiprinimo dviejų lėkių Nd:YAG stiprintuve

tyrimai. Nustatyta, kad sustiprinus plokščios gaubtinės impulsą iki ~8 kartų ir pasiekus išvadinės spinduliuotės intensyvumą iki $I_{0,5}=1,3 \text{ GW/cm}^2$ bei energijos srauto vertes iki $F_{0,5}=0,128 \text{ J/cm}^2$, stiprinamų impulsų forma matavimo paklaidų ribose nesikeičia.

Šeštajame skyriuje aprašyta disertacinio darbo metu sukurta pikosekundinė Nd:YAG stiprintuvų sistema didelės energijos OPCPA sistemos kaupinimui. Jos pirmąją pakopą sudaro du nuosekliai veikiantys lazerinio diodinio kaupinimo regeneraciniai stiprintuvai, kurie atlieka pradinį oscilatoriaus užkrato signalo stiprinimą ir kuriuose formuojami reikiamos trukmės ir kontrasto impulsai. Po to impulsai toliau stiprinami antroje sistemos pakopoje, kurią sudaro lempinio kaupinimo stiprintuvai, sustiprinantys impulsą iki 600 mJ energijos. Parametriniam kaupinimui reikalinga antrosios harmonikos spinduliuotė generuojama pakopiniuose antrosios harmonikos generatoriuose. Kartu realizuojamas išvadinių impulsų plokščios gaubtinės formavimo metodas. Sistema yra optiškai sinchronizuota su užduodančio femtosekundinio Yb:KGW oscilatoriaus impulsais, turi ~300 mJ, 75 ps trukmės Gauso impulsų ir 100 mJ, > 100 ps trukmės hipergausinės laikinės formos antrosios harmonikos impulsų išvadus

Paskutiniame skyriuje yra apibendrinami atliktų tyrimų rezultatai ir pateikiamos disertacijos išvados.

Brief information about the author

Name: **Jonas**
Last name: **Adamonis**
Date of birth: 1983.07.06
Place of birth: Šiauliai, Lithuania

Education

- 2008-2012: Vilnius University, Faculty of Physics, PhD;
- 2006-2008: Vilnius University, Faculty of Physics, Master degree (graduate) studies (“Laser Physics and Optical Technologies”);
- 2002-2004: Vilnius University, Faculty of Physics, Bachelor degree (undergraduate) studies (“Management of Modern Technologies”)
- 2002: finished Juliaus Janonio Gymnasium in Šiauliai.

Professional experience:

- 2005 till now: Engineer, UAB “Ekspla”.
- Participation in research projects “Paradigma”, “Integra”, “Naglis”.